

YF-12 PROPULSION RESEARCH PROGRAM AND RESULTS

James A. Albers and Frank V. Olinger
Dryden Flight Research Center

SUMMARY

The YF-12 propulsion research program was initiated to contribute to the technology base for the design of efficient propulsion systems for supersonic cruise aircraft. The research has been directed toward the following areas of technology: flight instrumentation, propulsion system steady state performance, propulsion system dynamic performance, propulsion system control, and airframe/propulsion system interactions. This report discusses the objectives and status of the propulsion program, along with the results acquired in the various technology areas. The instrumentation requirements for and experience with flight testing the propulsion systems at high supersonic cruise are discussed. Propulsion system performance differences between wind tunnel and flight are given. The effects of high frequency flow fluctuations (transients) on the stability of the propulsion system are described, and shock position control is evaluated. The report discusses present and future program plans and schedules.

INTRODUCTION

Supersonic cruise aircraft require propulsion systems that operate efficiently in a wide range of altitudes and at speeds from subsonic to high supersonic. To avoid penalties in engine size, weight, and fuel consumption, the inlet must supply air at maximum pressure and with minimum drag and interference. The inlet must also be able to match the airflow requirements of the engine over a wide range of flight conditions. Optimizing an inlet for a given aircraft mission requires an extensive investigation of the tradeoffs between optimum inlet performance at design and off-design conditions.

A first step in the optimization of the propulsion system is an analytical study of the various inlet geometries that match the engine requirements. Next, wind tunnel tests of scaled models are performed. These tests are followed by flight tests. It is known that, in general, wind tunnel test conditions do not exactly duplicate flight test conditions because for scaled models the Reynolds numbers and the local flow field do not always correspond to those experienced in flight. In addition, the instrumentation location and geometry of wind tunnel models are difficult to match to those of flight hardware. Because the flight hardware and its expected performance are determined from scaled wind tunnel models, scaling techniques that allow subscale inlet data to be extrapolated to full-scale flight are necessary.

Many of the current propulsion system problems of supersonic cruise aircraft involve inlet-engine compatibility. Insufficient propulsion system stability margin caused by instantaneous pressure distortion has been and continues to be a significant problem. It is at present not clear how the dynamic data from model tests should be used to predict the stability margin of the propulsion system in flight.

Another area of major concern to the propulsion system designer is the prevention of inlet unstarts, which occur in mixed-compression inlets when the terminal shock moves out in front of the cowl lip. Unstarts can take place when either internal disturbances or external disturbances occur in flight. New propulsion control concepts are needed to position the terminal shock in the inlet duct. At present, mixed-compression inlets have variable geometry features that are programmed by a variety of engine, inlet, and airframe variables. For example, in the YF-12 inlet, variable bypass doors and a spike or ramp move as functions of Mach number, angle of attack, normal acceleration, and angle of sideslip. New bleed systems and shock position sensors may be required to improve the response of the present control system.

Experience to date with supersonic cruise aircraft has indicated that strong interactions exist between the propulsion system and the flight control system. These effects have been traced to the porting of bleed and bypass flows overboard around the nacelle. This porting can result in separated flow on the external nacelle and in the base and boattail region surrounding the engine exhaust. Thus, the nacelle flow interactions of supersonic cruise aircraft require further investigation. An integrated aircraft control system is needed to minimize undesirable interactions of the inlet, engine, and airframe control systems.

The YF-12 propulsion research program was initiated to contribute to the technology base for the design of efficient propulsion systems for supersonic cruise aircraft. This program is a cooperative effort among the Dryden Flight, Ames, and Lewis Research Centers. The technology areas include flight instrumentation, propulsion system steady state performance, propulsion system dynamic performance, propulsion system control, and airframe/propulsion system interactions. The status of the YF-12 propulsion program in the first quarter of 1976 was reported in reference 1. This paper updates that report and gives some results in the areas of technology indicated above. The paper also discusses present and future program plans and schedules.

SYMBOLS

K_{θ}	circumferential distortion
K_{RAD}	radial distortion
M_{∞}	free-stream Mach number

m_0	reference captive mass flow
m_{cb}/m_0	centerbody bleed mass flow ratio
m_{eng}/m_0	engine mass flow ratio
m_{fwd}/m_0	forward bypass mass flow ratio
m_{st}/m_0	shock trap mass flow ratio
p_{t_0}	inlet local total pressure
p_{t_∞}	free-stream total pressure
\bar{p}_{t_2}	average compressor face total pressure
$p_{t_{2max}}$	maximum compressor face total pressure
$p_{t_{2min}}$	minimum compressor face total pressure
Δp_s	change in static pressure
r_c	reference cowl lip radius
ΔW	change in engine airflow
W_0	reference airflow
ΔW_{dis}	engine airflow decrement due to distortion
x	axial distance measured from spike tip when spike is full aft
α_0	local angle of attack relative to inlet centerline of symmetry
α_∞	free-stream angle of attack
β_0	local angle of sideslip relative to inlet centerline of symmetry
θ	circumferential angle measured from vertical centerline

OBJECTIVES AND APPROACH

The principal objective of the YF-12 propulsion program is to develop methods for the extrapolation of inlet dynamic performance characteristics from wind tunnel to flight. This involves determining the sensitivity of the propulsion system to such variables as scale, Reynolds number, and flow field entering the inlet. The inlet configurations and facilities used for this study are shown in figure 1. Reynolds number and scale effects can be evaluated by comparing 1/3-scale and full-scale inlet test results. In addition, the effects of aircraft forebody flow field on inlet performance can be evaluated by comparing wind tunnel inlet model data with flight results. By comparing wind tunnel and flight high frequency response data, scaling techniques can be developed that permit the extrapolation of subscale inlet dynamics to full-scale flight, and ways to use wind tunnel results for the prediction of flight performance can be established.

Another objective of the program is to determine the effects of high frequency flow fluctuations (transients) on the stability of the propulsion system and to evaluate new control concepts intended to minimize these effects. Wind tunnel models are used to investigate the effects of downstream disturbances on the dynamics of the propulsion system and to evaluate various shock position controls for mixed-compression inlets. Flight data can be used to determine the effects of both upstream and downstream disturbances, such as free-stream turbulence, on the stability of the propulsion system.

Another objective of the program is to investigate the causes of airframe/propulsion system interactions and to seek ways to minimize these effects. A control system is being developed to optimize total system performance by integrating the inlet, engine, and aircraft control systems.

Other objectives of the program include the determination of the operational range of the inlet for various geometries and flow conditions, the development of high temperature pressure sensors and other instrumentation for propulsion system testing, and use of the YF-12 airplane as a test bed for the investigation of new propulsion system concepts, such as the turbofan ramjet and variable cycle engine.

YF-12 PROPULSION SYSTEM DESCRIPTION

The propulsion system of the YF-12 airplane (fig. 2) consists of an axisymmetric mixed-compression inlet (fig. 3) and a J58 afterburning turbojet engine which exhausts through a convergent-divergent blow-in-door ejector nozzle. The inlet has a translating spike and uses a system of rotating forward and aft doors to control airflow. Throat bleed is provided by a porous slotted section on the spike and a combination flush slot and ram scoop on the cowl commonly referred to as a shock trap. The spike bleed air is ducted through struts and overboard through fixed louvers. The shock trap air is

ducted aft through the forward bypass plenum by the shock trap tubes and then ducted around the engine to the ejector nozzle. Each engine has a nine-stage single rotor compressor which is driven by a two-stage turbine. The main burner consists of an eight-can combustor. The engine is equipped with a fully modulating afterburner. The primary nozzle area is variable and is used to maintain the desired engine speed for both afterburning and nonafterburning operation. A more detailed description of the propulsion system and instrumentation is given in reference 2.

INSTALLATION OF FLIGHT INSTRUMENTATION

Inlet performance measurements on the YF-12 inlet rely primarily on pressure measurements. Steady state measurements can be used to evaluate the overall performance of the propulsion system. Considerable interest has developed in recent years in inlet-engine compatibility, scaling effects, and the evaluation of inlet transient performance. High frequency response pressure measurements are most useful for investigating these aspects of propulsion systems.

Installing the two types of transducers used in the YF-12 flight program (fig. 4) is difficult for several reasons. The size of the steady state (less than 100 Hz) transducer, although much greater than that of the high frequency response transducer, is not necessarily a problem because the space between the internal and external skins of the inlet is adequate for mounting purposes (fig. 5). However, attaching the tubing for the transducers at a static pressure port requires access to both sides of the internal skin, and this requires the removal of large portions of the external skin. Furthermore, not all of the internal skin of the inlet can be exposed, and this makes access to these areas difficult.

Most of the measurements used to evaluate inlet performance are made in the throat region. Structurally, this region is complicated by provisions for the throat bleed and bypass airflows, which are needed to control the position of the terminal shock wave. Experience with the YF-12 airplane has shown that the throat region is one of the most difficult to gain access to for instrumentation purposes.

The smaller size of the high frequency response transducer shown in figure 4 allows the transducer to be close coupled to the measurement location. This transducer has been used for both static and total pressure measurements. Figure 6 shows the total pressure rakes installed at the compressor face. The transducers are mounted in the rakes, and the pressure and signal lines are routed into the centerbody. The lines are then collected, forming a bundle which is routed through the struts, airflow passages, and part of the wing, where it finally terminates in a cooled bay. A schematic of the installation is shown in figure 7. Approximately 10.7 meters of line are needed to reach the signal conditioning units and data acquisition system, which must be kept in a

temperature-controlled environment. Because connectors are sensitive components, they are located in open areas and the number of connectors has been minimized. Three connectors were used for the YF-12 application, one close to the transducer and the other two in the wing bays. The routing shown in figure 6 also typifies the steady state transducers. Much of the wire routing requires working blind. In some parts of the inlet it has been necessary to cut holes in the structure to accommodate the instrumentation, but this procedure should be avoided if possible to maintain the structural integrity of the inlet.

PROGRAM RESULTS

Propulsion System Steady State Performance

Many steady state wind tunnel and flight data have now been obtained with the YF-12 inlet. The approximate number and location of the pressure sensors are shown in figure 8. The steady state data include measurements of pressure recovery, airflow (bleed, bypass, and engine), compressor face distortion, duct static pressure, inlet control duct pressure, and boundary layer pressure.

Wind tunnel and engine calibration results.—A 1/3-scale model of the YF-12 inlet was tested at Ames in the Unitary Plan Wind Tunnel at Mach numbers from 0.9 to greater than 3.0 and at Reynolds numbers based on the cowl lip radius between 1.2×10^6 and 4.0×10^6 . The aircraft's internal inlet geometry was completely simulated from the centerbody tip to the engine compressor face, including the variable forward and aft bypass doors and the centerbody and cowl bleed systems. The basic data are presented in references 3 and 4.

A full-scale flight inlet was tested in the Lewis 10'x10' Supersonic Wind Tunnel at Reynolds numbers based on the cowl lip radius between 2.0×10^6 and 4.2×10^6 . The wind tunnel installation is described in detail in reference 5, and the results are given in references 6 and 7.

As part of the effort to obtain accurate airflow measurements in flight, an engine airflow calibration was performed at the Lewis Research Center's Propulsion Systems Laboratory (ref. 8). The engine that was installed in the aircraft was calibrated with distortion screens, which produced distortion patterns that simulated flight conditions. The engine airflow decrement due to distortion was obtained by comparing this calibration to the airflow characteristic curve that represented an average engine with no distortion (fig. 9). A decrement of up to 4 percent in corrected engine airflow was obtained for a corresponding typical maximum-minus-minimum distortion level of 20 percent. This indicates that engine calibrations should be performed in ground tests with and without distortion screens to obtain accurate airflow measurements in flight.

The local flow conditions at the inlet plane in flight must be known in order to match them with wind tunnel conditions. Wind tunnel tests of a

1/12-scale model of the YF-12 aircraft were conducted in the Ames Unitary Plan Wind Tunnel to investigate local Mach numbers, total pressures, and flow angles for various free-stream Mach numbers, angles of attack, and angles of sideslip (ref. 9). The local flow angles and Mach numbers are illustrated in figure 10 at a free-stream Mach number of 2.75. The flow angles are presented as vectors, with the origin of each vector the point where the data were recorded. The vector is the resultant of the local flow angles, α_0 and β_0 , relative to the inlet centerline of symmetry. The lengths of the vector represent the magnitude of the resultant flow angle. Figure 10(a) indicates that the local flow changes from predominantly downwash at the low angles of attack to predominantly upwash at the higher angles of attack. In addition, there is a component of crossflow from outboard to inboard throughout the angle of attack range. Figure 10(b) indicates an increase in local Mach number gradient across the inlet plane with an increase in angle of attack. The Mach number gradient is as high as 0.14 at an angle of attack of 7.4° . The nonuniformities in inlet flow field and local Mach number, which are caused by the aircraft's forebody, could cause differences in the performance of the inlet in the wind tunnel and in flight. The wind tunnel test conditions correspond to the average of the flight test conditions at the inlet plane.

Flight test results.—Inlet performance was investigated in flight at Reynolds numbers based on the cowl lip diameter between 1.9×10^6 and 8.5×10^6 for various flight conditions and inlet geometries. The flight conditions tested were Mach number, angle of attack, and angle of sideslip. Inlet geometry was varied by changing the position of the forward bypass doors, the aft bypass doors, and the spike. The effects of these variables on pressure recovery, distortion, airflow, and shock position were investigated.

The pressure recovery and distortion at the compressor face are shown in figure 11 for nominal operating conditions. Pressure recovery varied from 97 percent at high subsonic Mach numbers to approximately 76 percent for supersonic conditions. Radial distortion (KRAD) and circumferential distortion (K θ) generally increased with Mach number. At low Mach numbers distortion was essentially radial. At higher Mach numbers, however, circumferential distortion predominated. The high levels of distortion are due primarily to flow angularity at the inlet face. Distortion patterns at various inlet conditions are discussed in detail in reference 10.

To illustrate the effects of airflow on inlet flight performance, various inlet airflow components are shown in figure 12 for a free-stream Mach number of 2.8. As the forward bypass doors close and the forward bypass mass flow ratio decreases, the engine mass flow ratio and recovery increase. The shock trap and centerbody airflows, which account for approximately 5 percent and 3 percent of the captured mass flow, respectively, do not change during the test.

The location of the terminal shock in the inlet duct can have a significant effect on the quality of flow entering the engine. The circumferential variations of shock position for three duct pressure ratios are shown in figure 13. Duct pressure ratio is the control parameter used to control shock position.

The peak static pressure turbulence level in the throat was used as the indicator of terminal shock position. The figure indicates considerable skewing of the terminal shock within the inlet. The largest shock movement due to changing the duct pressure ratio occurred on the inboard side of the inlet, with little or no movement occurring on the outboard side. Increasing the duct pressure ratio caused the inboard side of the terminal shock wave to move ahead of the geometric throat. The skewing of the terminal shock is influenced by the Mach number gradient and the flow angularity ahead of the spike (fig. 10). The sensitivity of the shock to these variables indicates that inlet orientation is critical in maximizing inlet performance for a supersonic cruise aircraft.

Wind tunnel/flight comparisons.—Every attempt was made to match the flow conditions and inlet geometry for the wind tunnel and flight tests. Usually, one or more of the variables (Mach number, angle of attack, angle of sideslip, bypass airflow, spike position, and engine airflow) could be matched, but matching all the variables was almost impossible. Preliminary comparisons indicated some differences between the wind tunnel and flight parameters, such as engine and centerbody airflow (ref. 11). More recent comparisons also illustrate the differences between 1/3-scale, full-scale, and flight data (fig. 14). The engine mass flow ratios obtained from the 1/3-scale and full-scale tests, which agreed, differed significantly with the ratio obtained in flight. The centerbody mass flow ratios obtained from all three sets of data (1/3 scale, full scale, and flight) differed widely. The differences between the wind tunnel and flight data could exist as shown in figure 14, or they could be due to unmatched inlet parameters.

To separate the two effects, a multiple regression model based on a least-squares criterion of YF-12 inlet performance parameters was derived from the full-scale wind tunnel data. This model provided a way to derive wind tunnel data for inlet conditions that matched the flight conditions. The multiple regression model gives equations (linear or nonlinear) of the dependent inlet performance variables in terms of the independent variables of the flow conditions and inlet geometry. The dependent variables are forward bypass mass flow ratio, duct pressure ratio, percent forward bypass door opening, engine mass flow ratio, shock trap mass flow ratio, centerbody mass flow ratio, and compressor face distortion. The independent variables are Mach number, spike position, angle of attack, angle of sideslip, corrected engine airflow, and compressor face recovery. A comparison of this model with the 1/3-scale, full-scale, and flight data is shown in figure 15. A comparison of the model (for the corresponding matched condition) with 1/3-scale, full-scale, and flight data indicates no difference in the engine mass flow ratios found; however, there are some differences between the centerbody mass flow ratios. The results in figures 14 and 15 indicate the need to compare wind tunnel and flight data at conditions that are actually matched (by using a common basis for comparison like a multiple regression model) to determine which differences in inlet performance parameters are real.

To sort out the differences between the wind tunnel and flight data for all the inlet performance parameters, the statistical technique called analysis of

covariance was then used. Analysis of covariance uses residuals (model-predicted minus actual) for both wind tunnel and flight data and considers the combined effect of all the performance parameters. By using this analysis one can determine whether a statistical difference exists between 1/3-scale, full-scale, and flight data. When all the performance parameters were considered together, an analysis of this type indicated no difference between the 1/3-scale, full-scale, and flight data. The data are being examined further to investigate differences in the individual variables.

Propulsion System Dynamic Performance

Wind tunnel results.—Large amounts of dynamic pressure data were acquired from 1/3-scale inlet tests at Ames and full-scale flight inlet tests at Lewis. The 1/3-scale data included data from a 40-probe total pressure survey at the engine face, duct wall static pressure measurements, and boundary layer total pressure measurements (fig. 8). A statistical analysis of some of these pressure data is given in reference 12. This study includes probability density and power spectral density curves but does not include instantaneous distortion calculations.

Dynamic pressure data from a full-scale flight inlet were obtained at Lewis. The pressure data included data from a 24-probe total pressure survey at the compressor face. The number of measurements and the measurement locations were identical to those used in the flight tests. These data were recorded on magnetic tape for comparison with the dynamic data to be obtained in the flight tests.

Flight test results.—A significant aspect of mixed-compression inlet performance is the response of the inlet to transients. The effects of several types of transients have been evaluated in flight. The evaluation included an investigation of the effects of deliberately induced unstarts and compressor stalls and also the effects of the wake of a passing supersonic aircraft.

A typical inlet unstart is shown in figure 16. The unstart was intentionally induced by slowly closing the bypass doors, forcing the terminal shock wave out of the throat. As the unstart begins, pressures downstream of the throat drop rapidly, while those upstream of the throat increase. It takes about 0.01 second for the shock to move all the way to the spike tip. The inlet control system then opens the bypass doors and translates the spike forward to restart the inlet. The restart occurs 0.5 second after the unstart. The unstart transient produces large airplane rolling and yawing moments and should be avoided if possible.

In order to define the maximum pressure in an inlet duct, a stall was induced in flight at high supersonic speeds by closing the manual bleed on the fourth stage of the compressor. Duct maximum pressure is extremely important for the definition of the inlet structural load requirements. A typical compressor stall time history is shown in figure 17. The compressor stall affects

the static pressures at the compressor face first, and then, as the shock propagates forward in the inlet, the static pressures upstream of the compressor face. The induced hammershock results in a considerable duct static pressure rise, as indicated by figure 17. As shown in figure 18, the maximum normalized increase in pressure occurs in the inlet throat. The increase in pressure varies throughout the inlet duct because of the inlet's area variation. A limited quantity of flight data is now available for comparison with analytical and semiempirical prediction techniques.

Two YF-12 airplanes were flown simultaneously in late 1975 to provide a chase situation for an experiment being tested on one of the airplanes. These flights provided an opportunity to investigate the effects of passing aircraft wakes on inlet performance. The instrumented inlet of the chase airplane was used to probe the wake of the lead airplane. The maneuvers were performed with the two aircraft approximately 164 meters apart at Mach 2.5 and at an altitude of approximately 1962 meters. The chase aircraft accelerated and decelerated in such a way as to cause the bow shock wave of the lead airplane to pass across the chase airplane at least twice. The pilot reported that the disturbances caused by passing in and out of the wake were mild and that no unstarts occurred. The pressure fluctuations measured at the nose boom of the chase airplane were small. The inlet control system did not respond to the disturbances because they were of such small amplitude and short duration. The free-stream disturbances had no detectable effect on the high frequency response pressure measurements in the inlet.

A significant problem in engine development is the provision of a sufficient stability margin to allow for dynamic pressure distortion. Current methods for determining the stability margin require extensive testing with a 40-probe rake at the engine face to insure inlet-engine compatibility, and this testing is highly complex and costly. An alternative, less expensive method for determining the extreme values of instantaneous inlet distortion is proposed in reference 13. This method estimates maximum instantaneous distortion from the steady state root mean square (rms) and power spectral density (psd) measurements of only a few compressor face total pressures. This method has previously been applied only to a limited amount of wind tunnel data. In figure 19, the values of maximum instantaneous distortion estimated with this method using data from only six pressure probes are compared with the values obtained by using all 24 probes in the rake array. In general, the agreement between predicted and measured values of instantaneous distortion is excellent.

Wind tunnel/flight comparisons.—The 1/3-scale, full-scale, and flight data are being digitized and distortion parameters are being calculated for selected wind tunnel/flight match points. The effects of filters, record length, engine rake configuration, boundary layer rakes, and distortion indexes are being investigated. The statistical characteristics of distortion indexes are being calculated to establish dynamic scaling laws for wind tunnel-to-flight correlations.

Propulsion Controls

A rather extensive wind tunnel inlet control program has been performed at Lewis to support the overall YF-12 effort. This program included a study of normal shock and duct pressure dynamics, the digital implementation of the actual inlet's forward bypass control system, the shock position sensors, experimental shock position controls, and the throat stability bleed control system. An engine temperature control system called a turbine inlet gas temperature (TIGT) control system was evaluated in flight. The standard forward bypass door control system was used during flight tests.

Wind tunnel test results.—Open loop dynamic wind tunnel data are given in reference 14, which evaluates the response of the flight inlet to internal airflow disturbances. A comparison of these wind tunnel data with a one-dimensional dynamic model of the inlet is shown in figure 20. The dynamic model is discussed in reference 15, and the analysis is extended to upstream flow field disturbances in reference 16. An examination of the figure indicates that phase agreement is excellent and that amplitude agreement is reasonable. These examples are typical of the agreement between the analysis and the experimental data.

The full-scale YF-12 flight hardware with the duct pressure ratio inlet control system was tested in the Lewis wind tunnel (ref. 17). The digital implementation of the inlet control system is shown in figure 21. Tests consisted of open loop and closed loop frequency responses and step transients. This investigation demonstrated that a digital computer could be used to implement all the schedules and meet all the other requirements of an actual aircraft inlet control system. The data obtained from these tests, which had a duct pressure ratio control system, served as the baseline for comparison with other shock position control systems.

Various shock position sensors were tested in the wind tunnel. One of those tested was a continuous-output shock position electronic sensor (ref. 18). The frequency response of this sensor is shown in figure 22. The response is excellent out to a frequency of 60 hertz. However, this sensor may be difficult to incorporate into the hardware for the inlet control, since it requires several pressure transducers to determine the terminal shock position over an operational range.

Results from frequency response and transient testing of various experimental shock position control systems are given in reference 19. For this investigation, optimal fixed form shock position controllers of the proportional-plus-integral form were used. One of the experimental controls used the shock position sensors described in reference 18 for the feedback signal. Both engine speed and forward bypass door position were used to control shock position. Although the optimal controllers gave better response than the aircraft's inlet shock position control, the system was limited by the response of the forward bypass door hardware.

One means of providing a greater stability margin for the control of shock position is to make the throat bleed function as a throat bypass by regulating

the bleed plenum exit area. A throat bleed control system of this type was designed for the YF-12 aircraft (fig. 23) and demonstrated in the wind tunnel at Lewis. In this system, bleed airflow is removed through a porous bleed region just ahead of the inlet shock trap. Two circumferential rows of mechanical relief valves control bleed plenum exit area and hence bleed airflow. The valves, instead of being actuated directly by the bleed plenum pressure, have a shield and duct to sense an actuating pressure. Such an arrangement provides better valve response to airflow disturbances for this application. The effects of downstream disturbances on the bleed system are given in reference 20. Although limited results of external effects are given in reference 20, such effects can best be investigated by flight testing. A comparison of the response of the standard forward bypass control with that of the forward bypass control modified with these stability valves is shown in figure 24. For low airflow disturbance rates (less than 5 percent per second) the standard inlet unstarts with a 10-percent change in airflow. The stability valves provide a considerable increase in stability margin, with a 20-percent change in airflow necessary to unstart the inlet for the range of airflow disturbance rates tested.

A flight program is planned for the near future to investigate the nature of atmospherically induced disturbances and their effects on mixed-compression inlets. If the results indicate that a shock stabilizing system is needed, it will then be desirable to demonstrate that the proposed systems are feasible in a flight environment and that mixed-compression inlets operate nearer peak performance with such systems.

Flight test results.—A turbine inlet gas temperature control system was designed and developed for the J58 engine and flown on the YF-12 aircraft. This control system has a high response fluidic sensor in which output is fed to the standard J58 exhaust gas temperature (EGT) controller (ref. 21).

The fluidic temperature sensor accumulated approximately 100 hours of flight time in the range of 1200 kelvins and 1500 kelvins. The sensor was subjected to the full range of operational environments, including unstarts and throttle transients. In addition, the signal from the fluidic sensor was used for closed loop control of the engine temperature for approximately 2 hours during the flight testing. The closed loop tests were conducted only for steady state conditions, since the system was not optimized for controlling the engine temperature throughout the full range of the flight environment. The sensor operated as predicted by the ground tests reported in reference 22, and visual inspection of the sensor following the flight tests revealed no deterioration.

Airframe/Propulsion System Interactions

As part of the YF-12 performance and propulsion program, a limited amount of information was obtained on nacelle flow interactions to lay the groundwork for future flight testing.

Wind tunnel test results.—Wind tunnel tests of a 1/12-scale model were run at Ames, primarily to obtain force data. A limited number of surface static

pressure measurements were obtained during these tests. The pressure orifices were installed on the left wing and nacelle, and measurements were made with various bleed flows through the forward bypass and centerbody bleed louvers.

Subsequent testing was done with the same model to obtain loads data. Many additional pressure orifices were installed for those tests. Extensive data were obtained throughout the Mach number range and for various bleed flows. In addition, data for started and unstarted inlet conditions were recorded.

Flight test results.—To obtain an understanding of the complex flow around the YF-12 inlet in flight, tufts were placed on the inboard upper and lower quarters of the nacelle (ref. 23). High-speed cameras were used to film the flow patterns revealed by tuft movement and direction. Flow patterns were obtained for a wide range of flight conditions. The effect of forward bypass door position on the local flow around the upper surface of the nacelle is shown in figure 25. Three general types of flow could be observed from the activity of the tufts. In steady flow, the tufts were nearly motionless and lay close to the surface. In unsteady flow, the tufts oscillated slowly, with small angles of movement. In turbulent flow, the tufts oscillated rapidly, with large angles of movement. Figure 25(a) shows the nacelle flow with the forward bypass door closed. The surface flow downstream of the top bypass exit on the upper nacelle was generally turbulent. When the doors were opened 20 percent (fig. 25(b)), an area of lateral and reverse flow appeared upstream of the topmost door. However, the bypass flow apparently injected enough energy into the boundary layer to eliminate flow separation downstream of the exit. When the bypass doors were 70 percent open (fig. 25(c)), the flow downstream of the top exit remained turbulent or became separated despite the strong flow through the exit. This study indicates that the exit louvers should be designed to minimize separated flow regions on the nacelle in order to minimize external drag.

Program Plans and Schedule

The present YF-12 propulsion program (table I) includes plans to complete the flight testing being done to obtain compressor face and duct dynamic data. These flights, which began in mid-1976, are being performed primarily for matching wind tunnel test conditions and for investigating the effects of transients on inlet performance. In addition, dynamic data are to be obtained for investigating the effects of free-stream turbulence. The propulsion program is to be followed by a cooperative airframe/propulsion control system program, which is to be concurrent with flight tests for evaluating advanced shock sensors and nacelle flow interactions.

Compressor face and duct dynamics.—The objectives of the compressor face and duct dynamic pressure flight tests are to obtain dynamic pressure data with the flight and inlet parameters matched with wind tunnel settings.

The flight and wind tunnel data are to be compared to establish dynamic distortion scaling laws. In addition, the dynamic pressure instrumentation should provide data for evaluating inlet transients, such as unstarts. The dynamic data are to be used to evaluate the causes and effects of the inlet transients, and the results are to be compared with analytical prediction techniques for aircraft stability and control. The dynamic pressure measurement instrumentation includes 24 compressor face total pressure sensors and 40 duct static pressure sensors with frequency responses from steady state to 500 hertz (fig. 8).

Atmospheric effects.—Some flight tests are to be made to measure and evaluate the effects of atmospherically induced turbulence on the dynamics of mixed-compression inlets. A gust probe is to be installed on the nose boom of the YF-12 airplane, and measurements of the free-stream turbulence are to be correlated with the dynamics of the inlet flow (including boundary layer measurements in the inlet). Data from these flight tests should be valuable for the determination of realistic inlet control design criteria and for comparison with inlet performance predictions.

Cooperative control.—Strong interactions between the airframe and the propulsion systems of supersonic cruise aircraft can cause significant penalties in terms of performance, range, fuel consumption, and structural weight. The development of an integrated control system that maximizes favorable interactions and minimizes unfavorable interactions is a complex control problem. Recent innovations in flight-qualified digital computers make them ideally suited for this problem because of their speed and accuracy and because digital control is so flexible.

The cooperative control program planned for the YF-12 airplane utilizes the integrated digital control concept and is to be flight tested in two phases. The purpose of the first phase is to validate the hardware and software required to convert the existing analog systems to digital control. The systems to be converted are the autopilot, air data system, inlet control system, and autothrottle. In the second phase, these systems are to be integrated and new control laws are to be developed using optimal as well as classical control methods. A complete description of this program is given in reference 24.

Advanced shock sensor.—In current inlet control systems, terminal shock wave position is inferred from a duct pressure ratio that is independent of altitude effects. However, the value of the duct pressure ratio reference must be scheduled to accommodate various operating conditions. Sensing the shock position directly would be advantageous because it would allow closed loop control of the shock position or other primary variable, eliminate the need for normalized signals, lead to tighter control with potentially higher inlet recovery, and eliminate or greatly simplify schedules.

Studies are now being made to evaluate various logic schemes for detecting shock position from static pressures measured in the shock operating region. The schemes could be implemented on the aircraft by using instrumentation already available and the cooperative control computer. Alternatively, data

could be recorded during flight tests for evaluation in a ground-based facility. Digital pressure transducers using fiber-optic technology should ultimately replace conventional transducers. Digital fiber-optic devices are attractive because they are passive and because signals are transmitted as light (on or off) to electronics mounted off the inlet. In addition, the use of fiber-optic cables eliminates electrical wiring and the associated electrical noise. A device using digital transducers and the logic indicated by wind tunnel and bench tests is then to be evaluated on the YF-12 airplane. The flight testing should determine the accuracy and reliability of the approach in the flight environment. If successful, the device could then be used for control purposes.

Nacelle flow interactions.—Bleed and bypass airflows that are dumped overboard from the inlet create a complex flow field which can adversely affect the stability and control of the airplane. Flight tests are to be made to obtain pressure data for the external nacelle and wing. The flight data are to be compared with pressures measured on a wind tunnel model. The data should result in a better understanding of the flow field and permit the methods used to predict these interactions to be evaluated.

REQUIREMENTS AND RECOMMENDATIONS FOR FURTHER PROPULSION SYSTEM RESEARCH

Future supersonic cruise aircraft propulsion systems must meet demanding environmental and performance standards. Recent propulsion system studies have selected two variable cycle engine concepts that appear to be capable of meeting these standards. Hardware development and component testing are underway to lead to experimental engines that incorporate these concepts. New nacelles and supersonic inlets that match the airflow requirements of the engines must be designed and tested. The inlets and engines can be ground tested separately under simulated flight conditions, but the integrated inlet-engine combination will require flight testing.

The YF-12 airplane could be used as a test bed for flight testing the new propulsion concepts. As illustrated in figure 26, this aircraft is capable of carrying full-scale propulsion system experiments that are independent of the aircraft propulsion system. This method of flight testing provides an opportunity to investigate the high risk aerodynamic and propulsion system concepts that are needed for the development of technically feasible and economically competitive propulsion systems. Realistic flight environments can be obtained over a continuous range of Mach numbers to provide performance information not obtainable in ground facilities.

Noise suppression continues to be a major concern for future propulsion systems. Quiet nozzles are to be developed as part of the new engine program, however, and they can be tested separately from the rest of the propulsion system. Such nozzles can be tested on the J58 engine, which has the high pressure ratio representative of advanced engines. Flight tests

should provide information on forward velocity effects, which are known to reduce the effectiveness of the noise suppressor relative to the static performance.

Before accurate performance predictions for supersonic cruise aircraft can be made, wind tunnel performance must be extrapolated to flight conditions. The data obtained from the YF-12 propulsion program should prove to be valuable for this purpose. An understanding of the causes of and ways to reduce instantaneous dynamic distortion is vital if inlet-engine compatibility is to be obtained. The YF-12 program should shed some light on this problem in aircraft development. If propulsion system performance is to be optimized, new shock sensors and shock position controls must be developed. The latest developments in this area have been and will continue to be pursued in the YF-12 propulsion program. Finally, the only way to optimize total aircraft performance is to design a control system (such as the cooperative control on the YF-12 airplane) which integrates the inlet, engine, and airframe control systems. It is imperative that representatives of the various disciplines of aircraft design (aerodynamics, structures, propulsion, and stability and control) work together to create an integrated aircraft design that is competitive economically and performs well.

REFERENCES

1. Albers, James A.: Status of the NASA YF-12 Propulsion Research Program. NASA TM X-56039, 1976.
2. Burcham, Frank W., Jr.; Montoya, Earl J.; and Lutschg, Phillip J.: Description of YF-12C Airplane, Propulsion System, and Instrumentation for Propulsion Research Flight Tests. NASA TM X-3099, 1974.
3. Anderson, J. Thomas; Martin, Robert K.; and Shibata, Harry H.: 1/3 Scale Inlet Model Test Results. Vol. I - Test Definition and Steady State Data Presentation. NASA CR-114702, 1974.
4. Anderson, J. Thomas; Martin, Robert K.; and Shibata, Harry H.: 1/3 Scale Inlet Model Test Results. Vol. III - Test Definition and Steady State Data Presentation. NASA CR-114704, 1974.
5. Lewis Research Center: Wind-Tunnel Installation of Full-Scale Flight Inlet of YF-12 Aircraft for Steady-State and Dynamic Evaluation. NASA TM X-3138, 1974.
6. Cubbison, Robert W.: Wind Tunnel Performance of an Isolated Full-Scale YF-12 Inlet at Mach Numbers Above 2.1. NASA TM X-3139, 1976.
7. Cubbison, Robert W.: Effects of Angle of Attack and Flow Bypass on Wind-Tunnel Performance of an Isolated Full-Scale YF-12 Inlet at Mach Numbers Above 2.075. NASA TM X-3140, 1976.
8. Ladd, J. M.: Airflow Calibration of a J-58 Engine at Simulated Supersonic Conditions. NASA TM X-71797, 1975.
9. Olinger, Frank V.; Shibata, Harry; and Albers, James A.: Local Flow Measurements at the Inlet Plane of a 1/12-Scale Model of the YF-12C Airplane. NASA TM X-3435, 1976.
10. Taillon, Norman V.: Steady-State Inlet Recovery and Distortion of the YF-12C Airplane. NASA TM X-3382, 1976.
11. Smeltzer, Donald B.; Smith, Ronald H.; and Cubbison, Robert W.: Wind Tunnel and Flight Performance of the YF-12 Inlet System. AIAA Paper 74-621, July 1974.
12. Anderson, J. Thomas; and Edson, Ralph D.: 1/3 Scale Inlet Model Test Results. Vol. II - Dynamic Data Analysis. NASA CR-114703, 1974.
13. Melick, H. Clyde; Ybarra, Andres H.; and Bencze, Daniel P.: Estimating Maximum Instantaneous Distortion From Inlet Total Pressure RMS and PSD Measurements. NASA TM X-73,145, 1976.

14. Cole, Gary L.; Cwynar, David S.; and Geysler, Lucille C.: Wind-Tunnel Evaluation of the Response of a YF-12 Aircraft Flight Inlet to Internal Airflow Perturbations by Frequency-Response Testing. NASA TM X-3141, 1974.
15. Willoh, Ross G.: A Mathematical Analysis of Supersonic Inlet Dynamics. NASA TN D-4969, 1968.
16. Cole, Gary L.; and Willoh, Ross G.: Analysis of the Dynamic Response of a Supersonic Inlet to Flow-Field Perturbations Upstream of the Normal Shock. NASA TN D-7839, 1975.
17. Neiner, George H.; Arpasi, Dale J.; and Dustin, Miles O.: Wind-Tunnel Evaluations of YF-12 Aircraft Inlet Control System by Frequency-Response and Transient Testing. NASA TM X-3142, 1975.
18. Dustin, Miles O.; Cole, Gary L.; and Neiner, George H.: Continuous-Output Terminal-Shock-Position Sensor for Mixed-Compression Inlets Evaluated in Wind-Tunnel Tests of YF-12 Aircraft Inlet. NASA TM X-3144, 1974.
19. Neiner, George H.; Seidel, Robert C.; and Arpasi, Dale J.: Wind-Tunnel Evaluation of Experimental Controls on YF-12 Aircraft Flight Inlet by Frequency-Response and Transient Testing. NASA TM X-3143, 1975.
20. Cole, Gary L.; Dustin, Miles O.; and Neiner, George H.: A Throat-Bypass Stability System for a YF-12 Aircraft Research Inlet Using Self-Acting Mechanical Valves. NASA TM X-71779, 1975.
21. Webb, William L.; and Reukauf, Paul J.: Development of a Turbine Inlet Gas Temperature Measurement and Control System Using a Fluidic Temperature Sensor. AIAA Paper 73-1251, Nov. 1973.
22. Webb, W. L.: Turbine Inlet Gas Temperature Measurement and Control System. AFAPL-TR-73-116, Air Force Aero Propulsion Laboratory, Wright-Patterson Air Force Base, Dec. 1973.
23. Yanagidate, Craig: Tuft Study of the Local Flow Around the Nacelle of the YF-12A Airplane. NASA TM X-56035, 1975.
24. Reukauf, Paul J.; Burcham, Frank W., Jr.; and Holzman, Jon K.: Status of a Digital Integrated Propulsion/Flight Control System for the YF-12 Airplane. AIAA Paper 75-1180, Sept. 1975.

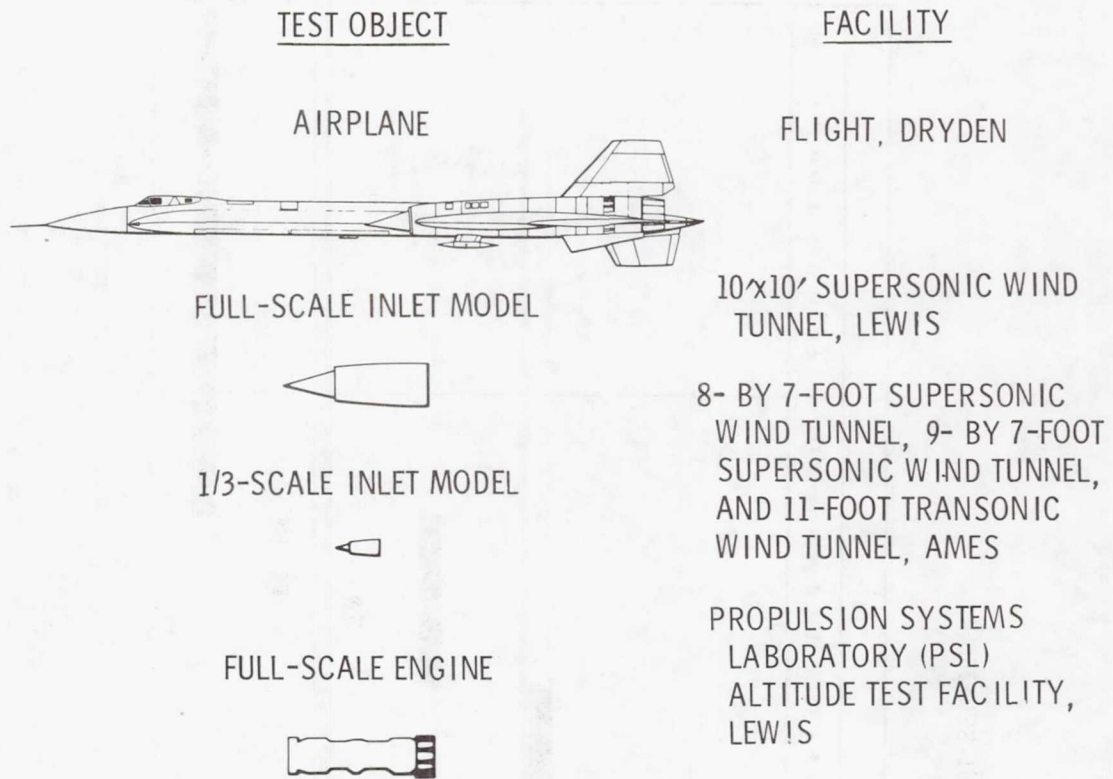


Figure 1.- Comparison of inlet configurations and facilities.

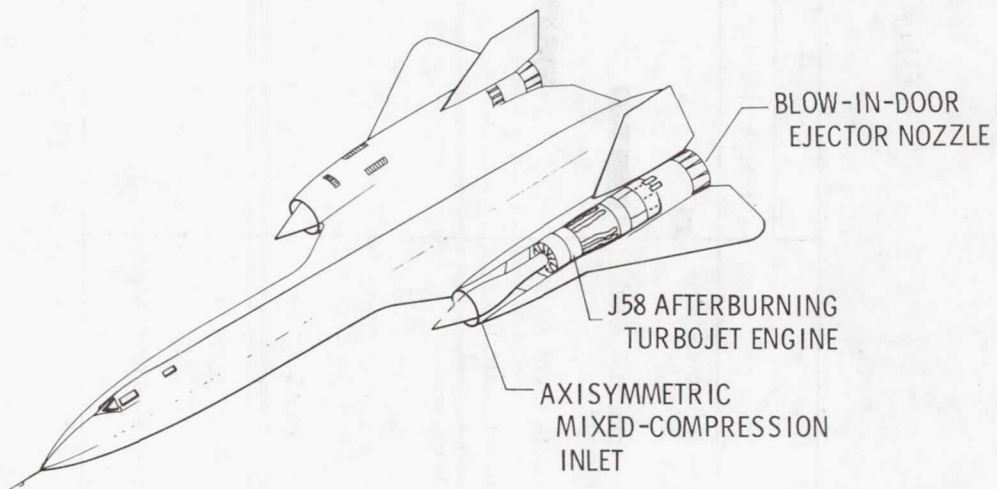


Figure 2.- YF-12 propulsion system.

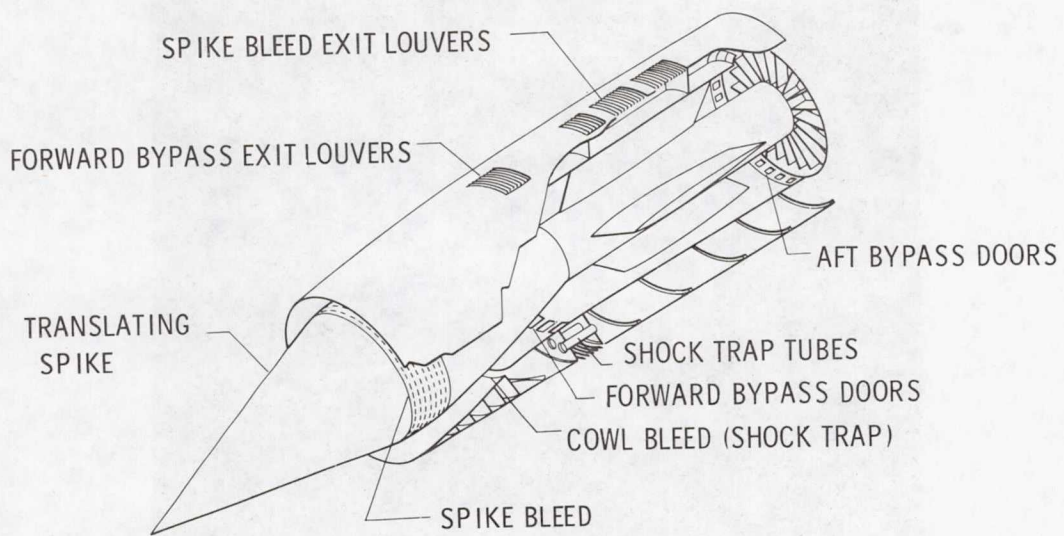


Figure 3.- YF-12 inlet.

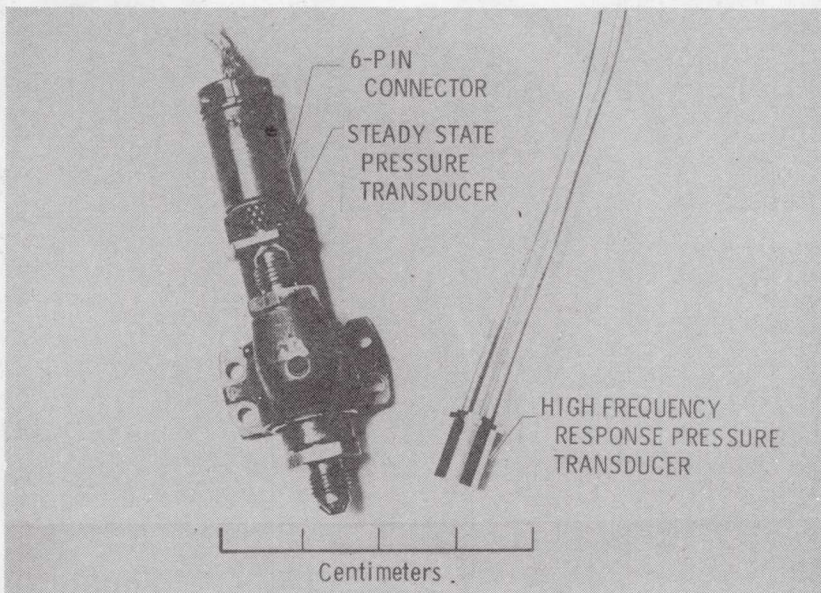


Figure 4.- High temperature pressure transducers used on YF-12 airplane.

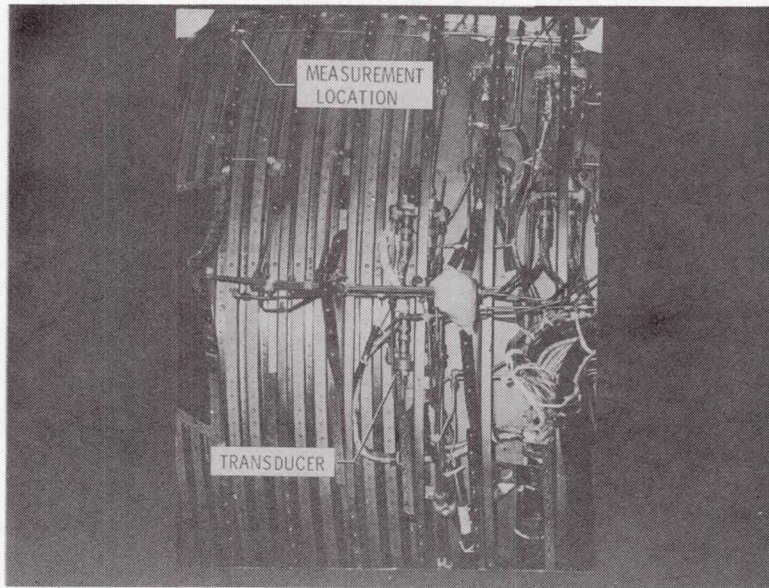


Figure 5.- Left inlet steady state pressure instrumentation (external skin removed).

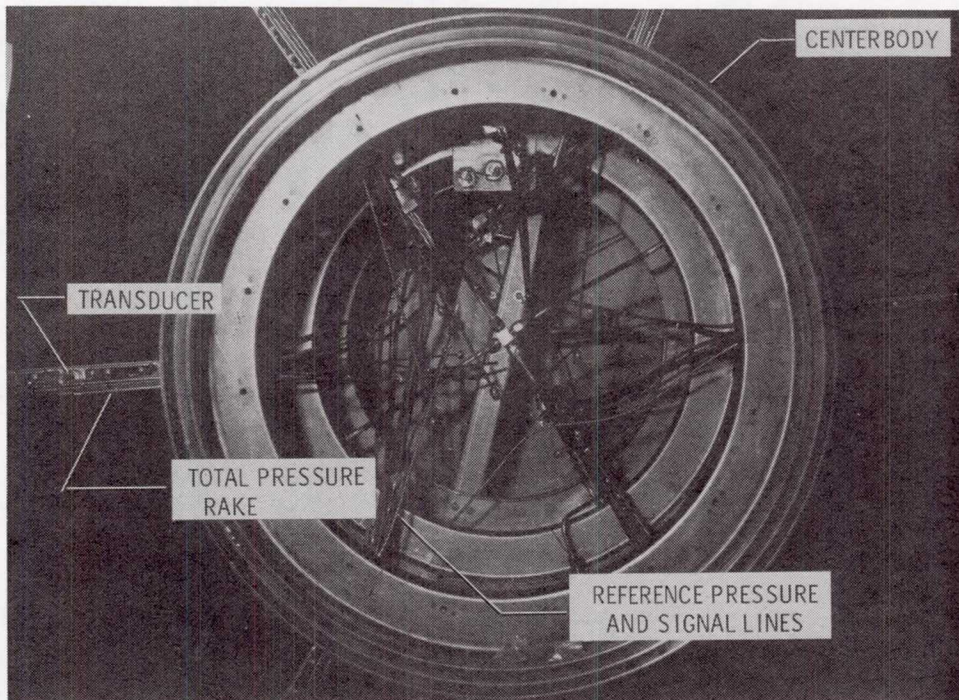


Figure 6.- Compressor face high frequency response pressure instrumentation (view looking forward).

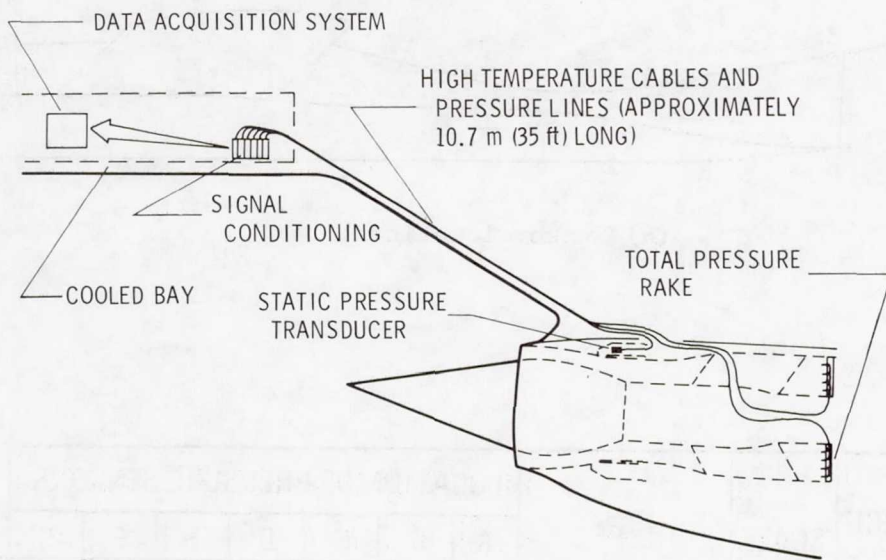
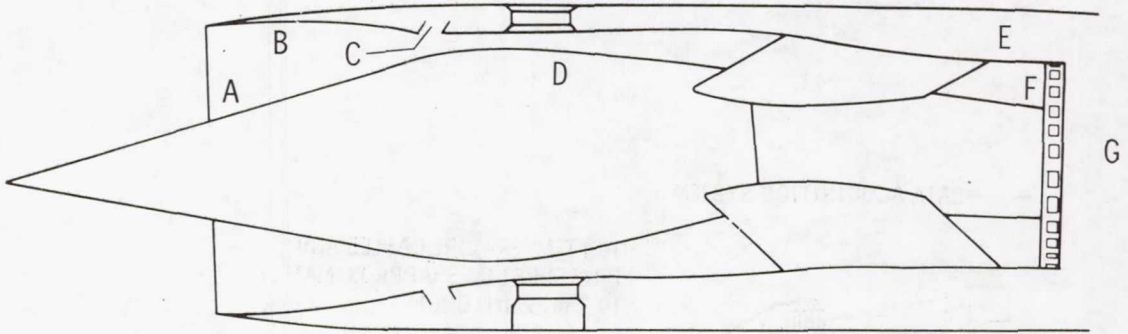


Figure 7.- Typical pressure instrumentation installation.

- A FORWARD SPIKE
- B FORWARD COWL
- C COWL THROAT
- D SPIKE THROAT
- E BLEED FLOW PASSAGE
- F COMPRESSOR FACE
- G ENGINE



(a) Sensor locations.

NASA RESEARCH CENTER	SCALE	TYPE	LOCATION OF PRESSURE SENSORS							TOTAL
			A	B	C	D	E	F	G	
			NUMBER OF SENSORS AT LOCATION							
AMES (WIND TUNNEL)	1/3	STEADY STATE	73	32	84	44	47	40	-	320
		DYNAMIC	12	6	16	12	1	40	-	87
LEWIS (WIND TUNNEL)	FULL	STEADY STATE	75	58	128	94	45	52	-	452
		DYNAMIC	-	11	27	-	12	24	-	74
DRYDEN (FLIGHT VEHICLE)	FULL	STEADY STATE	9	17	32	8	13	50	3	133
		DYNAMIC	4	4	19	6	6	24	3	66

(b) Number of sensors.

Figure 8.- YF-12 inlet study instrumentation comparison.

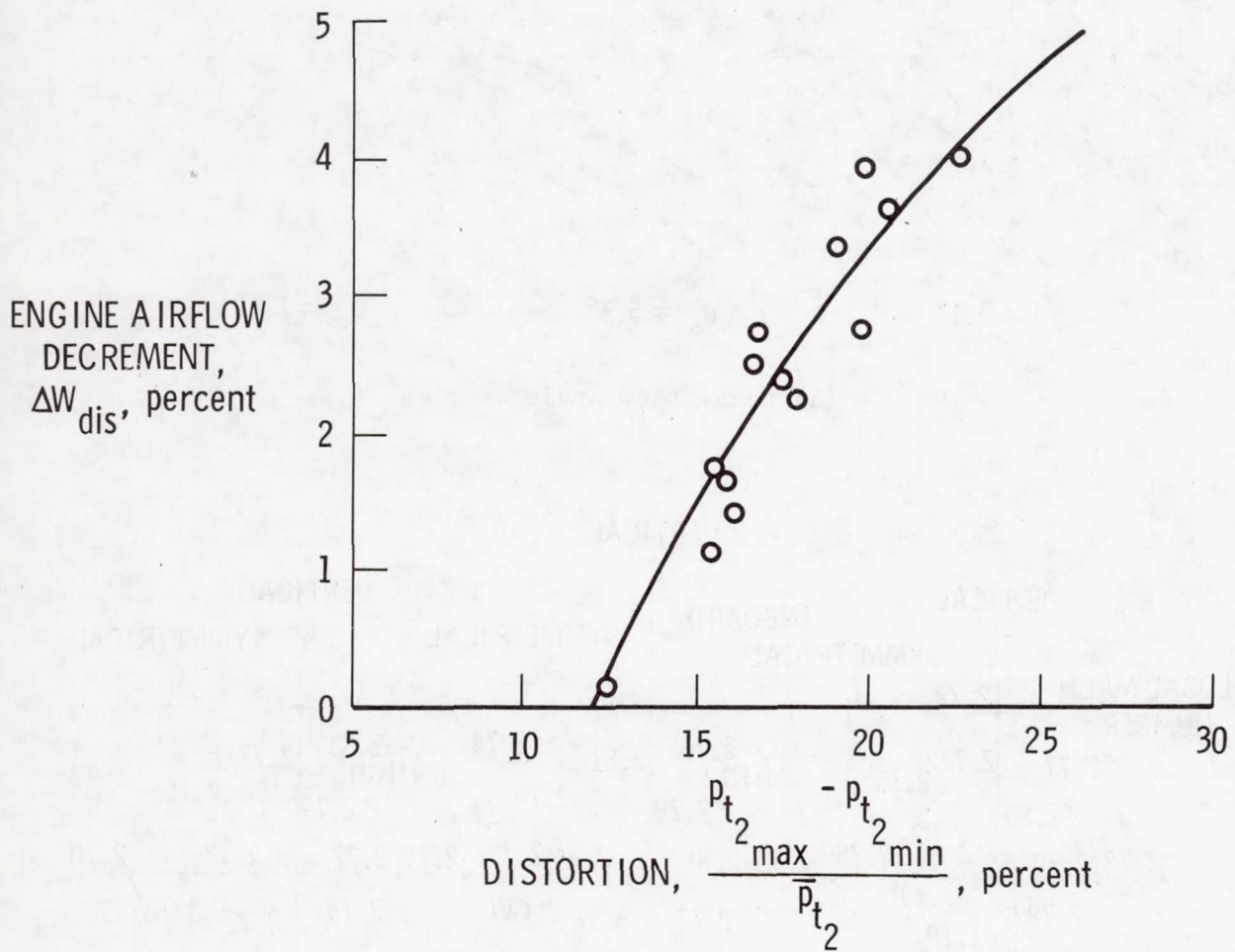
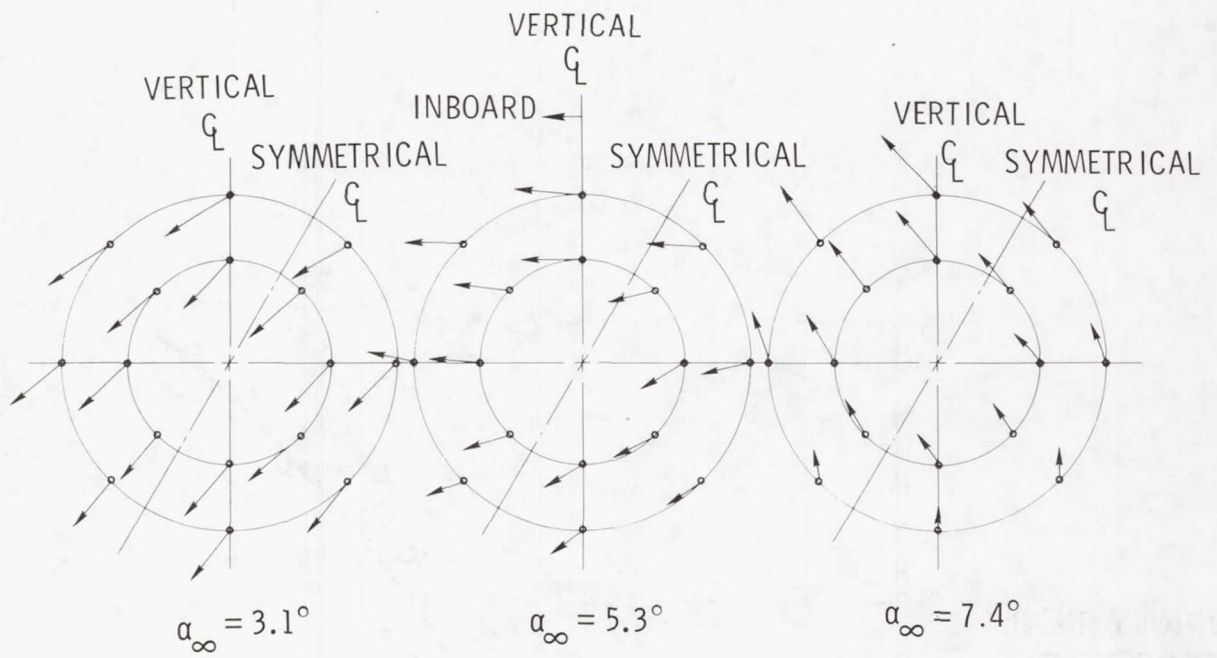
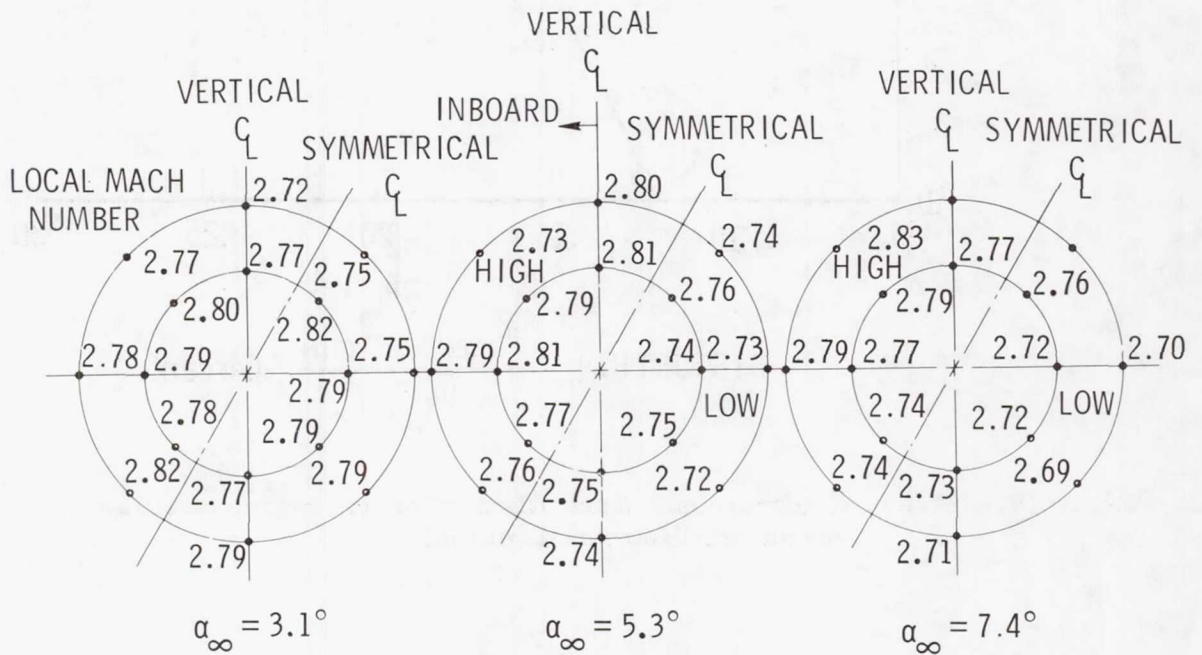


Figure 9.- Effect of compressor face distortion on engine airflow (engine airflow calibration).



(a) Local flow angle.

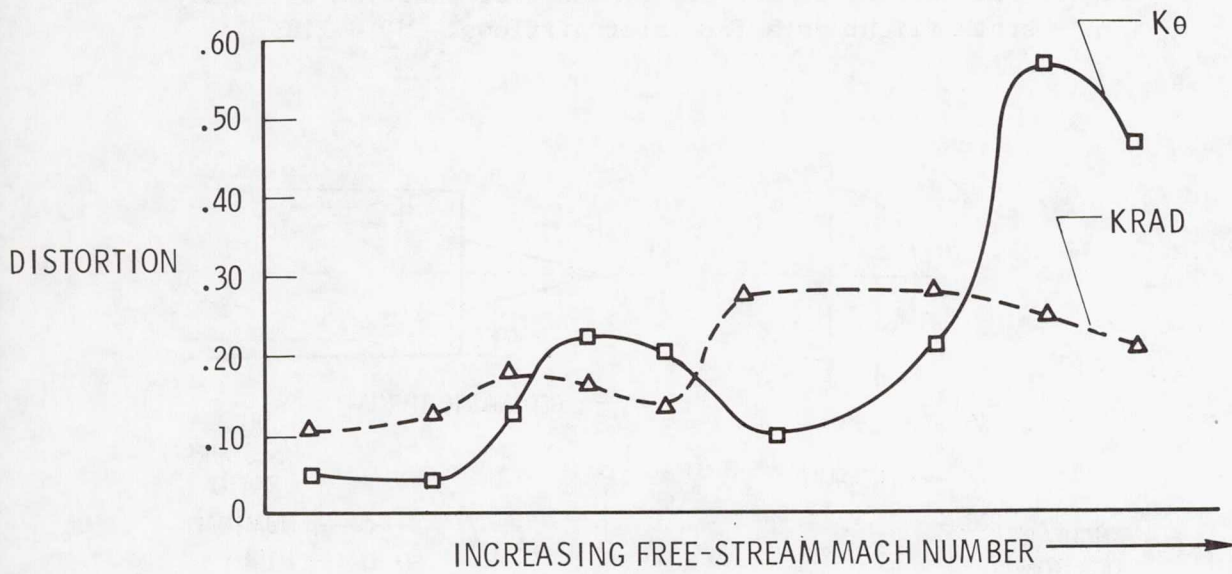


(b) Local Mach number.

Figure 10.- Local flow conditions at inlet plane of 1/12-scale model of YF-12 airplane. $M_\infty = 2.75$.



(a) Recovery.



(b) Distortion.

Figure 11.- Steady state flight data of pressure recovery and distortion at compressor face.

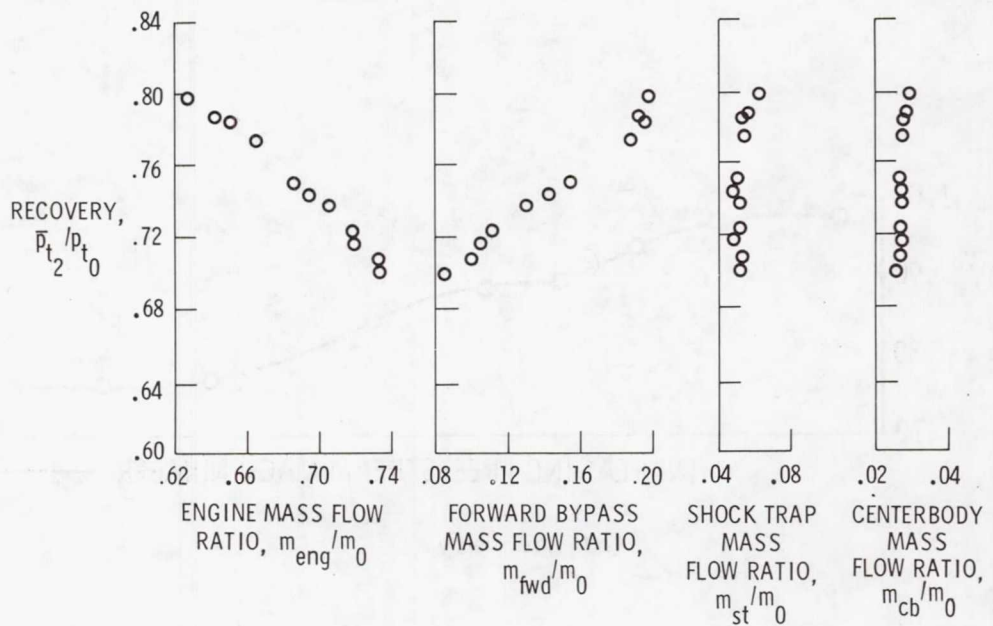


Figure 12.- Effect of forward bypass door position on steady state flight data for inlet airflows. $M_\infty = 2.8$.

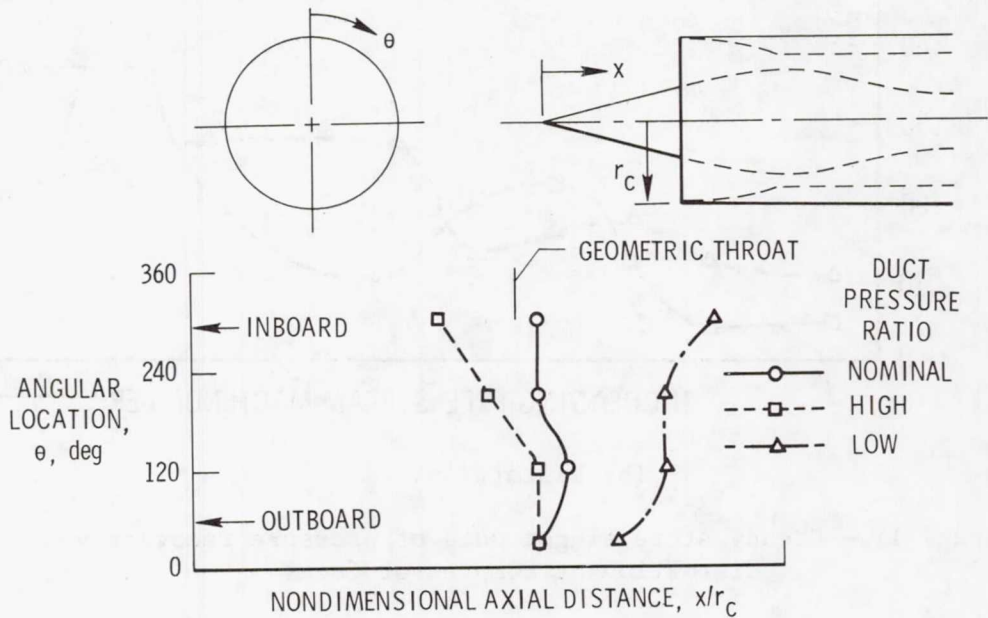


Figure 13.- Circumferential variation of shock position for three duct pressure ratios. $M_\infty = 2.8$.

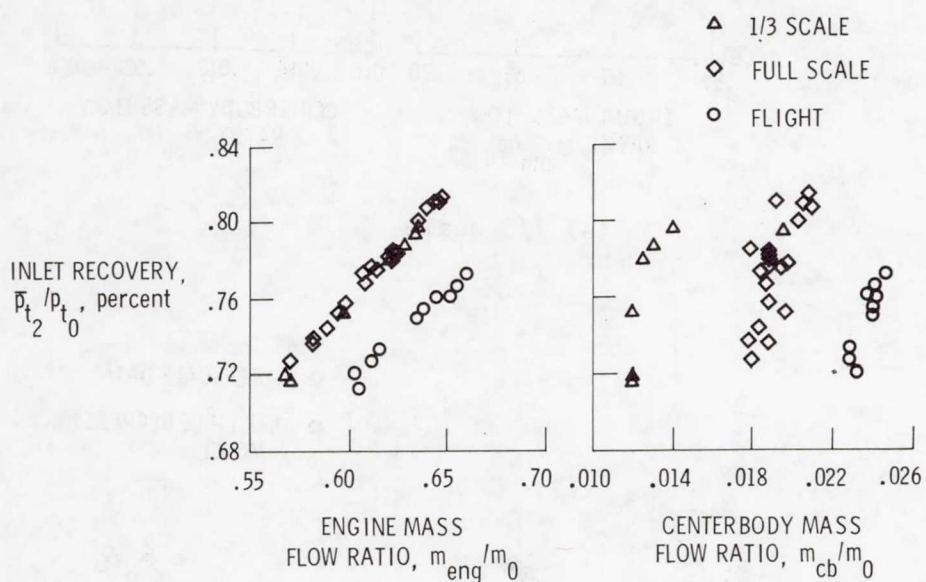
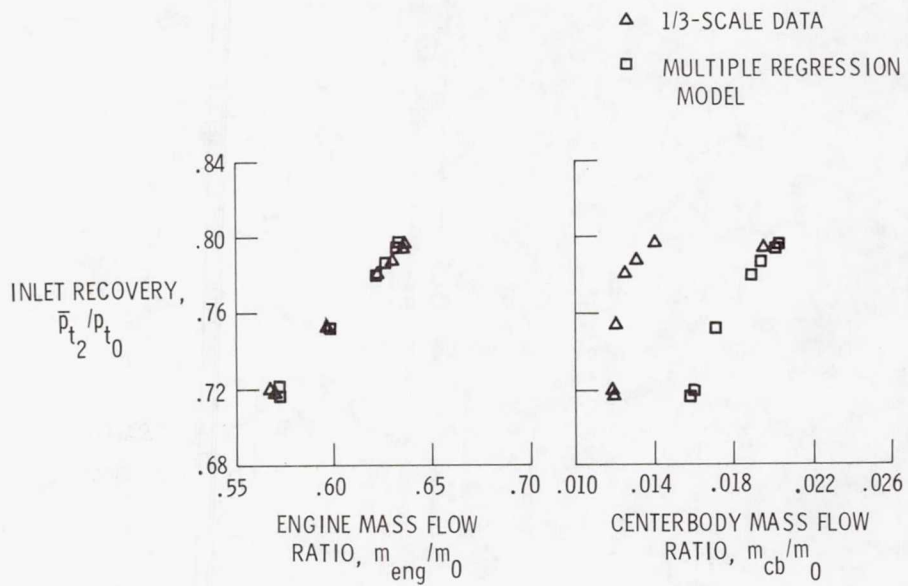
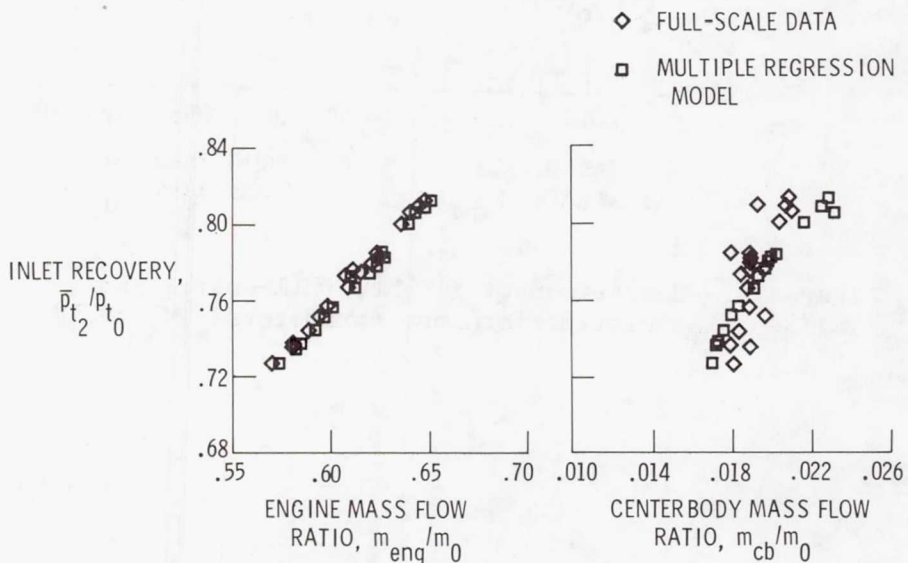


Figure 14.- Comparison of flight, full-scale, and 1/3-scale inlet performance parameters. $M_\infty = 2.8$.

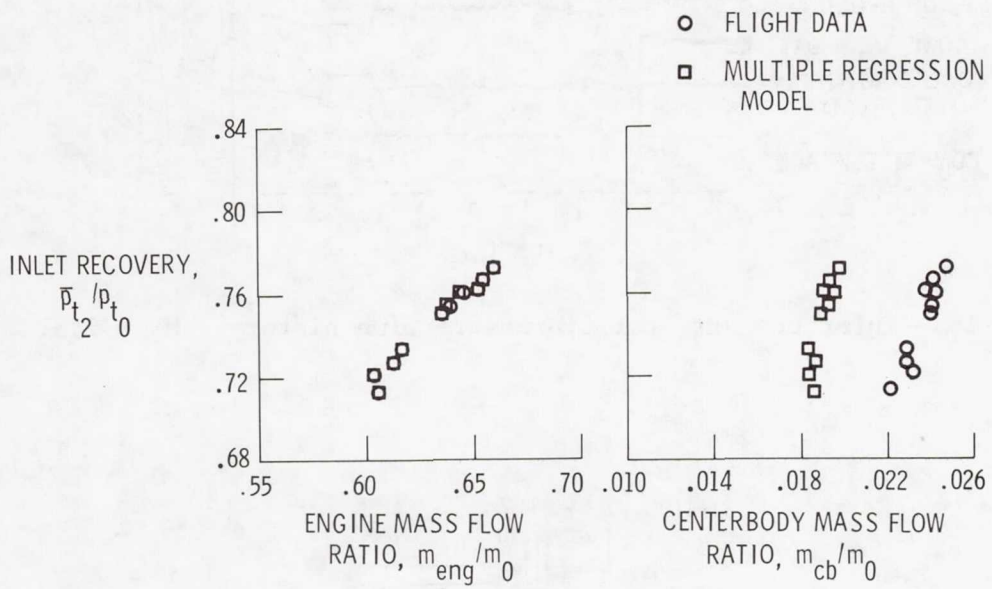


(a) 1/3 scale.



(b) Full scale.

Figure 15.- Comparison of multiple regression model with 1/3-scale, full-scale, and flight inlet test results. $M_\infty = 2.8$.



(c) Flight data.

Figure 15.- Concluded.

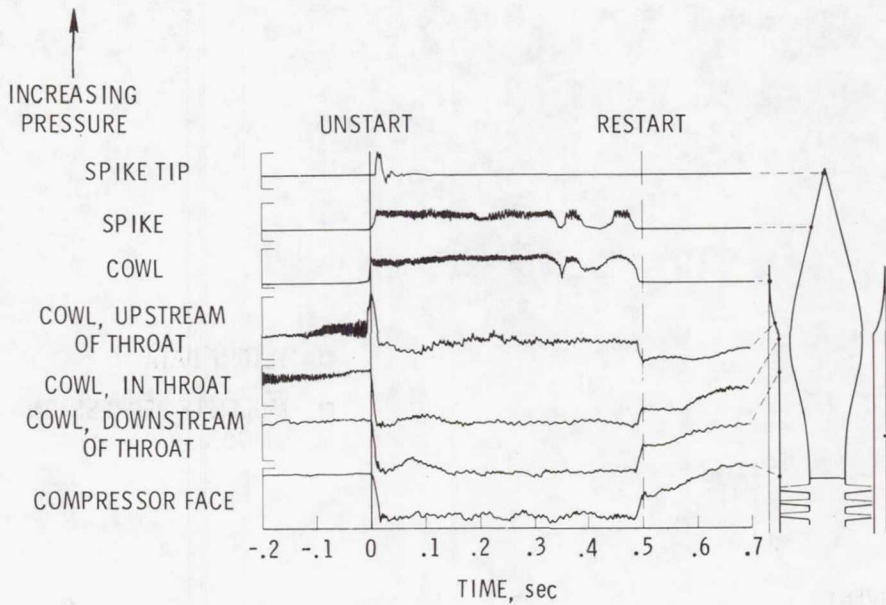


Figure 16.- Inlet unstart static pressure time history. $M_\infty = 2.5$.

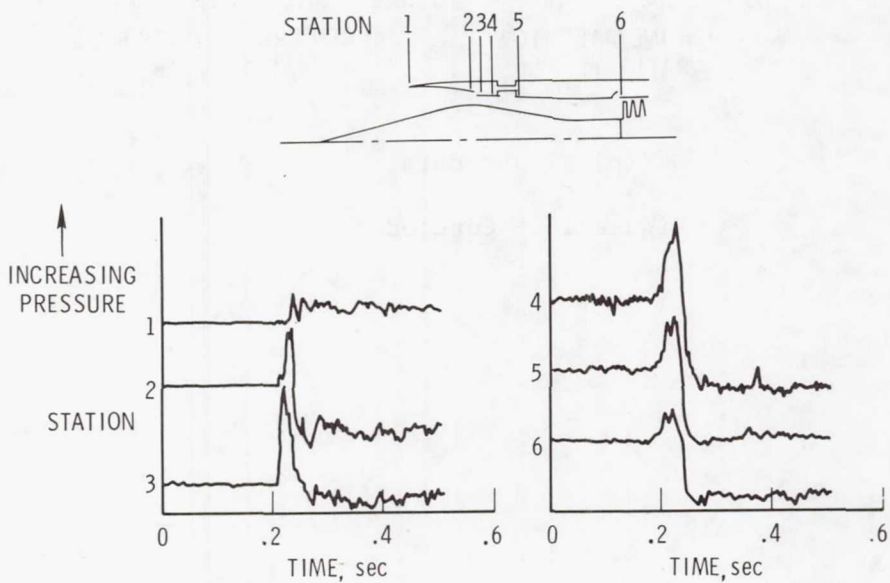


Figure 17.- Compressor stall duct pressure time history.

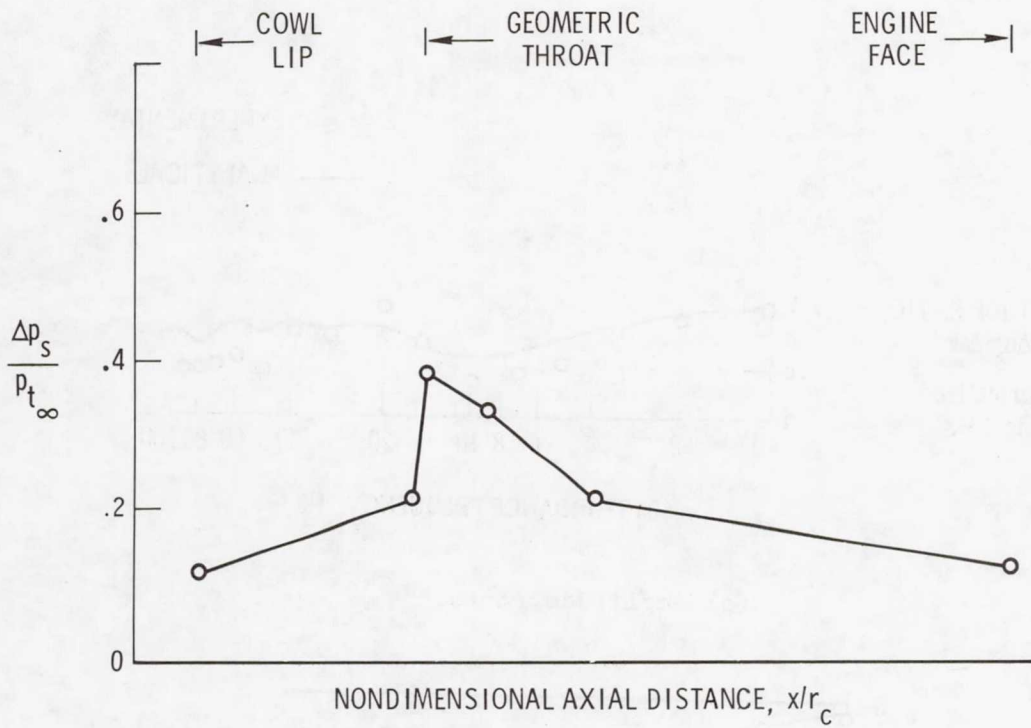


Figure 18.- Duct pressure rise during compressor stall.

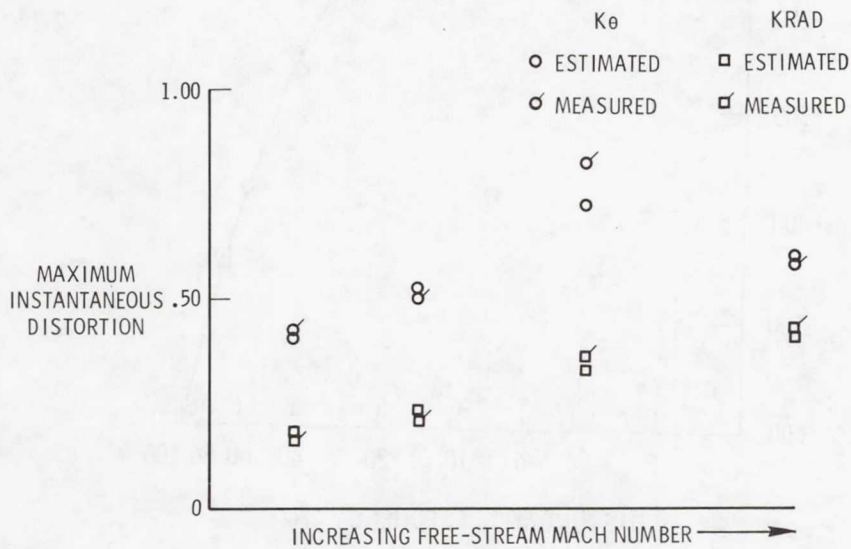
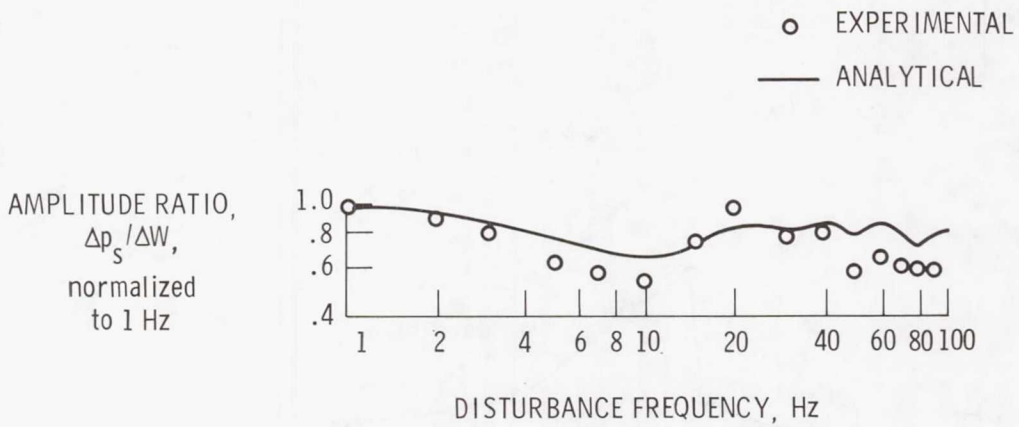
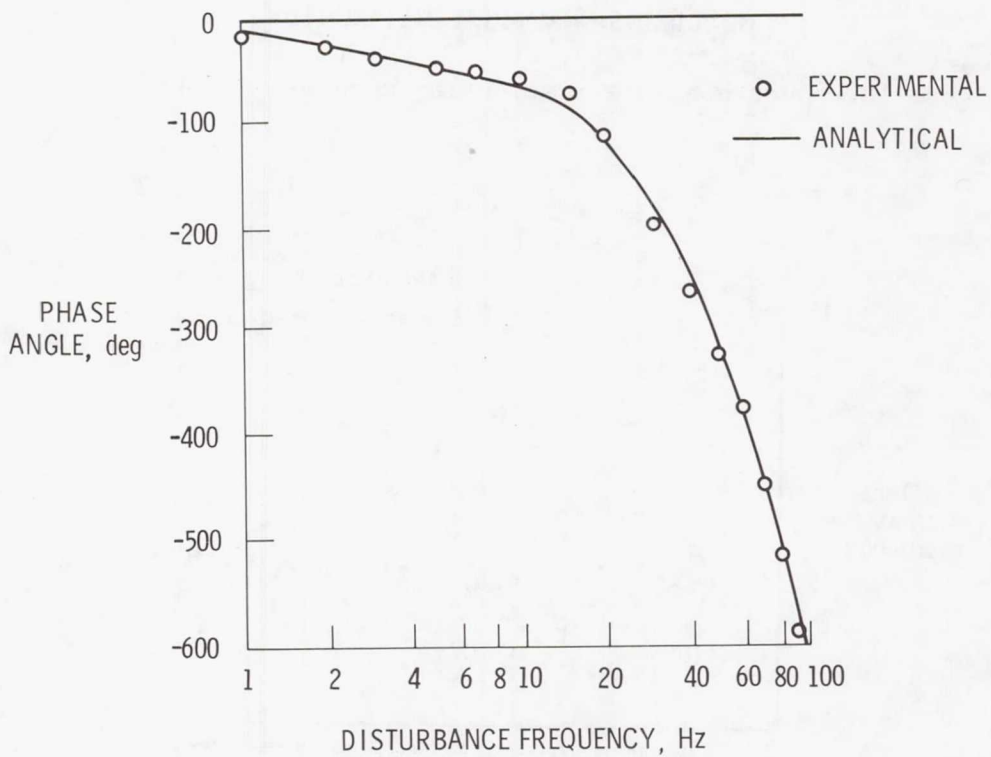


Figure 19.- Comparison of flight-measured with estimated maximum instantaneous distortion. Estimates are from inlet rms and psd measurements.



(a) Amplitude ratio.



(b) Phase angle.

Figure 20.- Comparison of inlet dynamic model and wind tunnel phase angle and amplitude ratio.

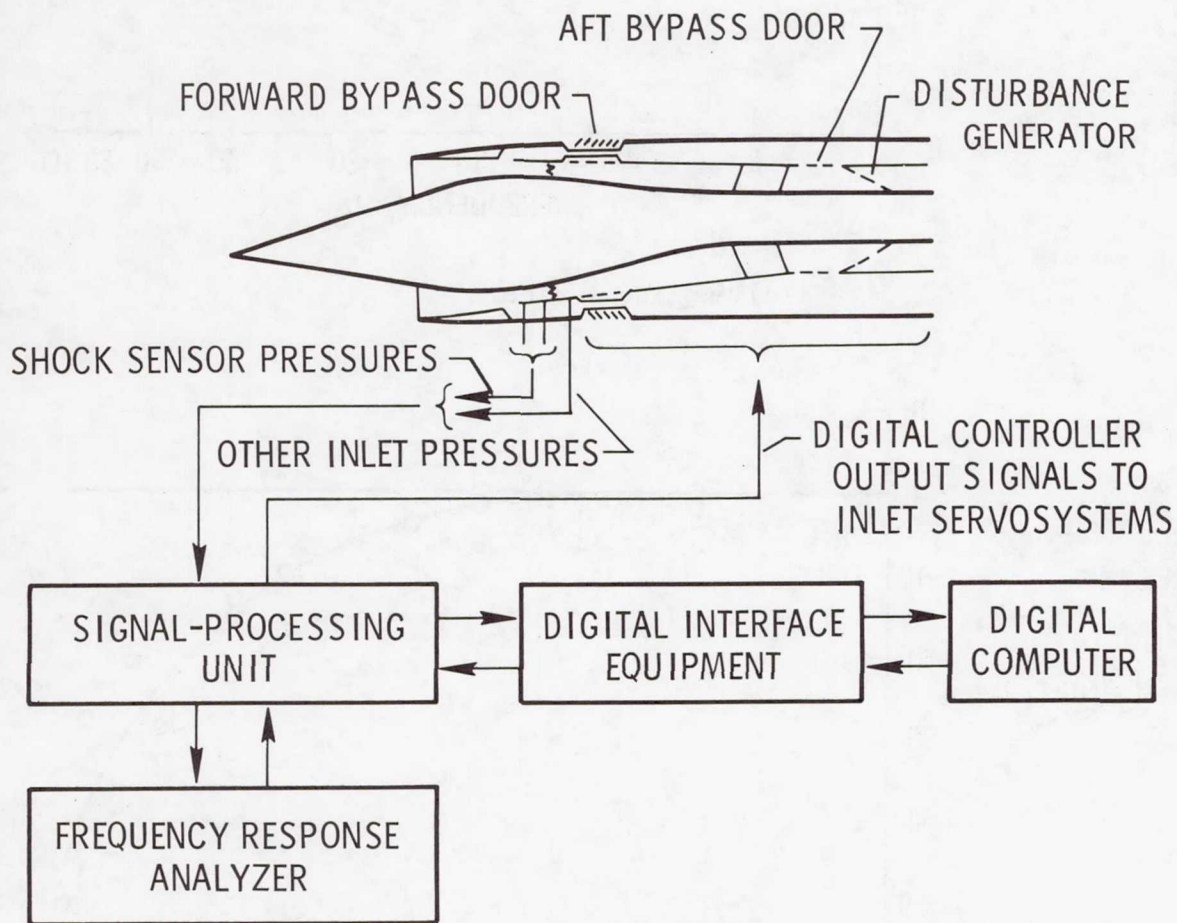
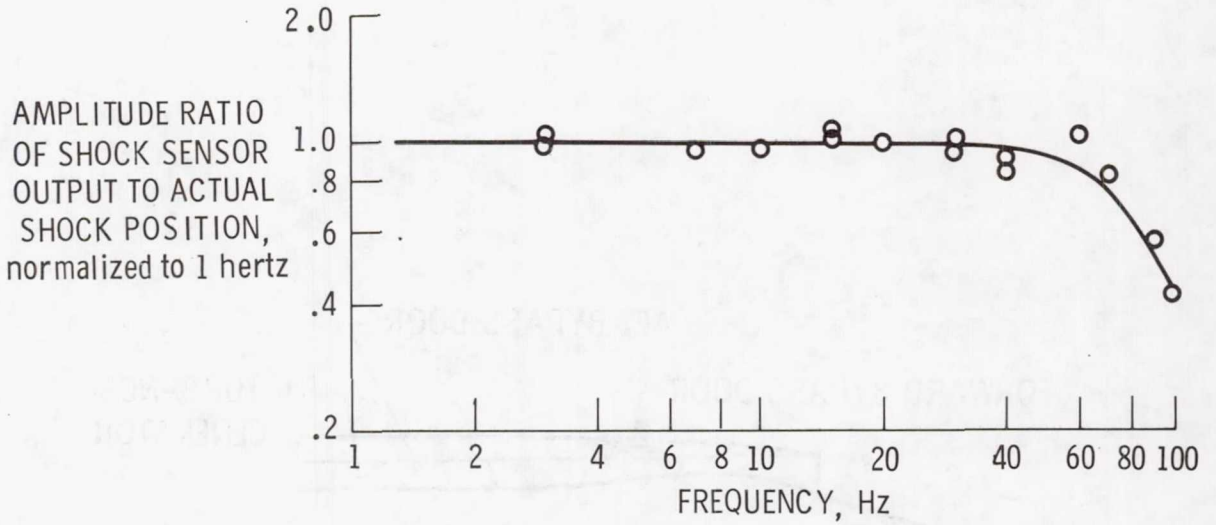
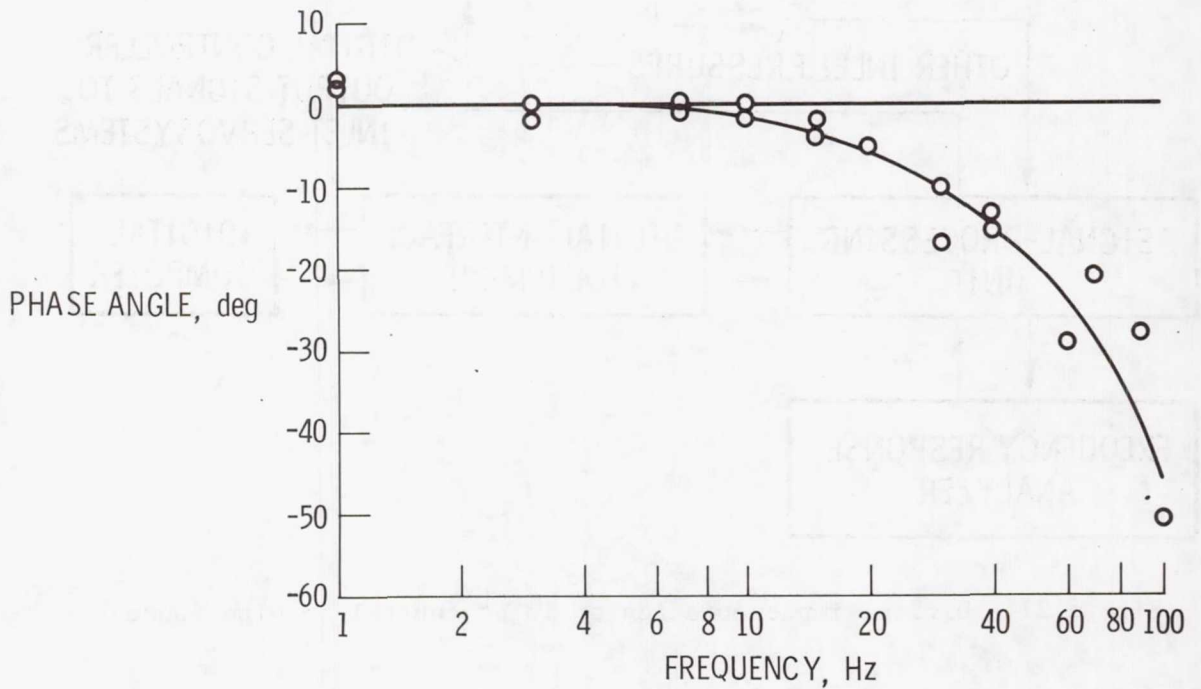


Figure 21.- Digital implementation of inlet control in wind tunnel.



(a) Amplitude ratio.



(b) Phase angle.

Figure 22.- Frequency response of terminal shock sensor output to actual shock position for continuous output electronic sensor.

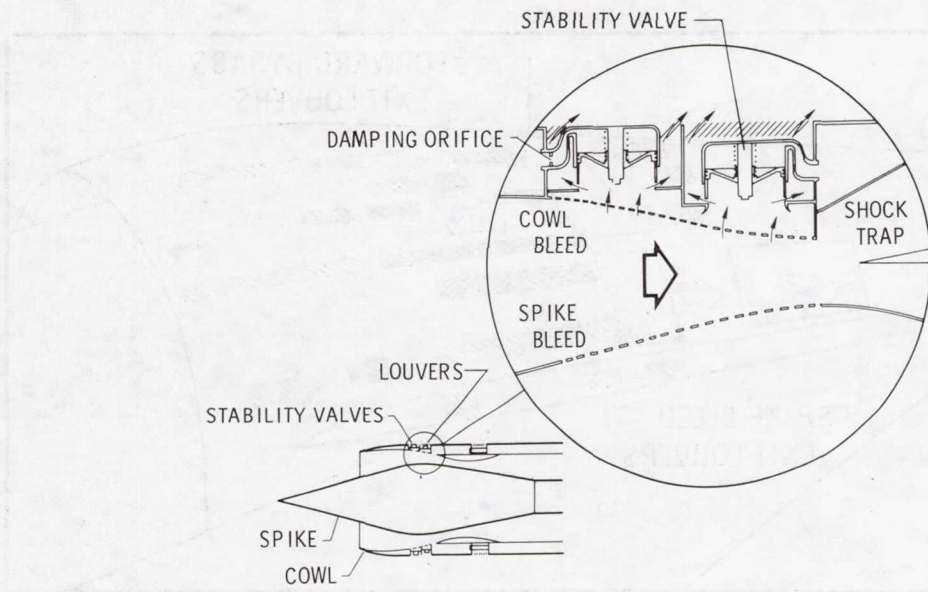


Figure 23.- Inlet configuration showing detail of stability valve installation.

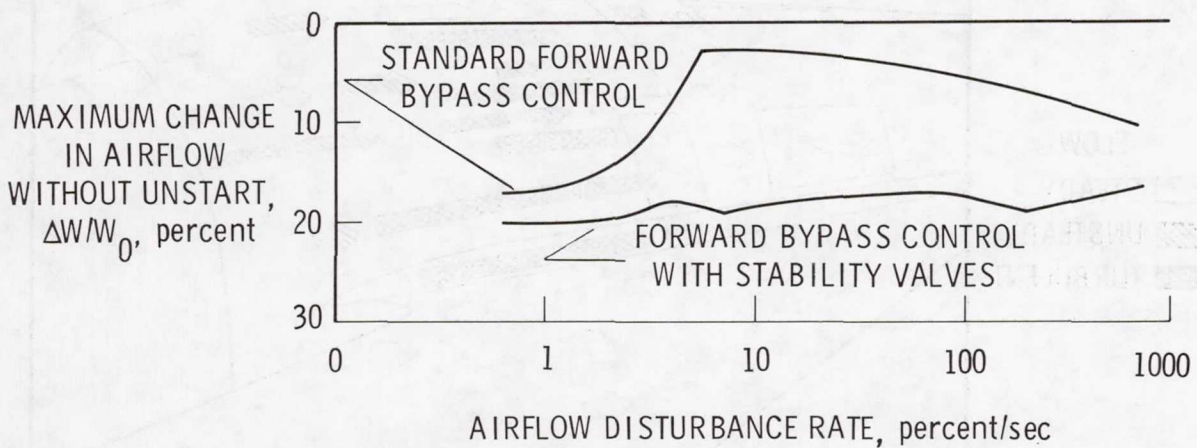
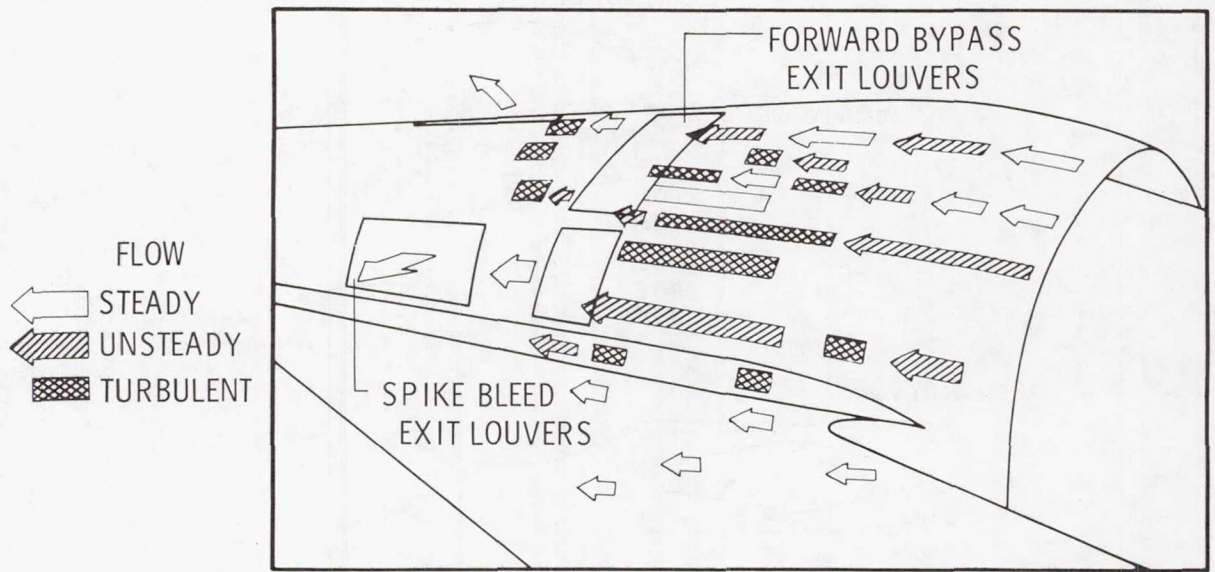
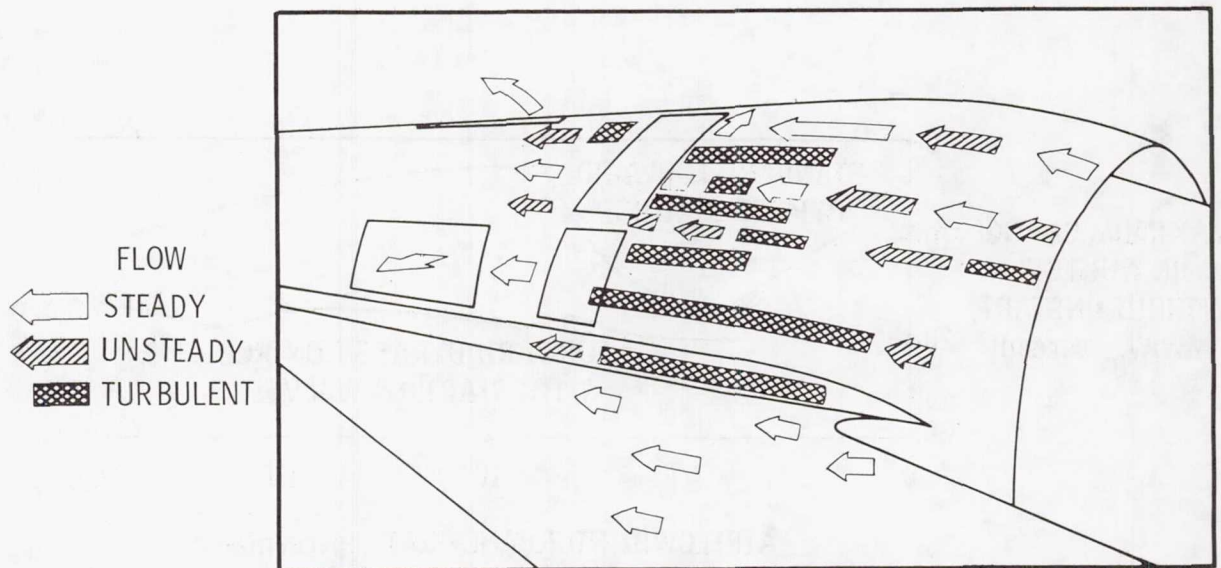


Figure 24.- Comparison of modified and standard inlet tolerance to internal airflow transients. $M_\infty = 2.5$.

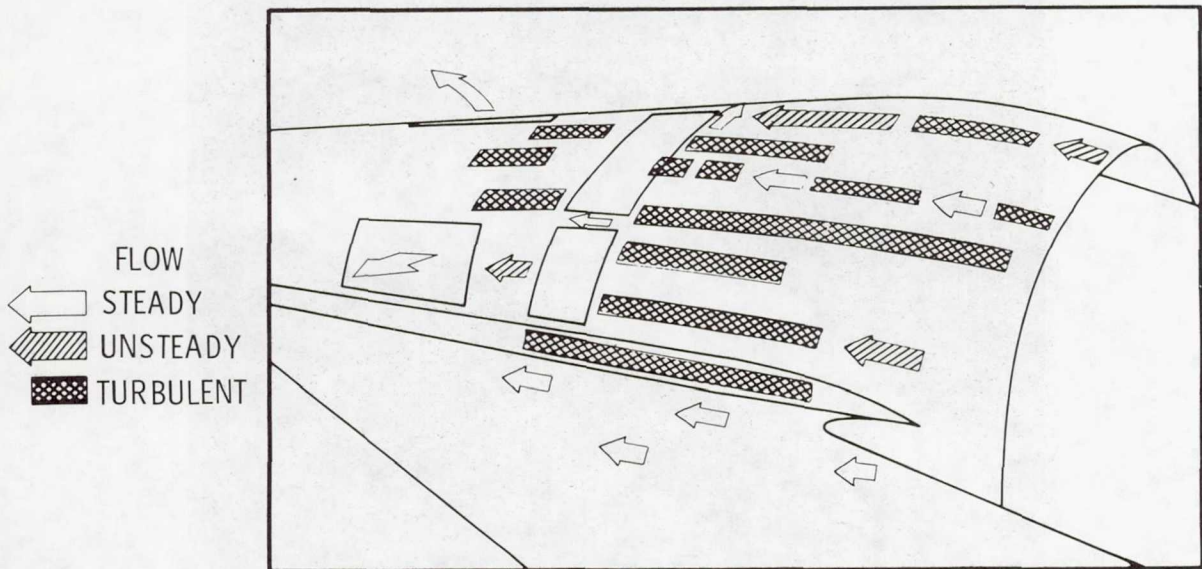


(a) Doors closed.



(b) Doors 20 percent open.

Figure 25.- Effect of forward bypass door position on local flow around nacelle. $M_\infty = 2.6$.



(c) Doors 70 percent open.

Figure 25.- Concluded.

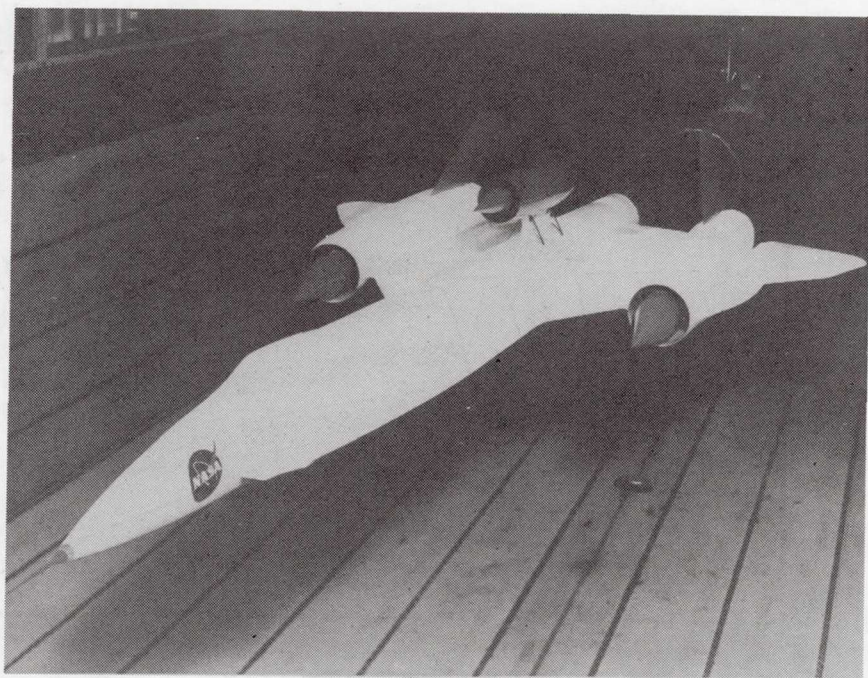


Figure 26.- YF-12 airplane as test bed for new propulsion concepts.